FORSCHUNGSZENTRUM ROSSENDORF

Mitglied der Wissenschaftsgemeinschaft Gottfried Wilhelm Leibniz

WISSENSCHAFTLICH-TECHNISCHE BERICHTE

FZR-353

August 2002

ISSN 1437-322X

Hans-Georg Willschütz, Eberhard Altstadt

Generation of a High Temperature Material Data Base and its Application to Creep Tests with French or German RPV-steel

Herausgeber:
Forschungszentrum Rossendorf e.V.
Postfach 51 01 19
D-01314 Dresden
Telefon +49 351 26 00
Telefax +49 351 2 69 04 61
http://www.fz-rossendorf.de/

Als Manuskript gedruckt

FORSCHUNGSZENTRUM ROSSENDORF
WISSENSCHAFTLICH-TECHNISCHE BERICHTE
FZR-353
August 2002

Hans-Georg Willschütz, Eberhard Altstadt

Technical Report / Sachbericht

Generation of a High Temperature Material Data Base and its Application to Creep Tests with French or German RPV-steel

Erzeugung einer Materialdatenbasis für hohe Temperaturen und ihre Anwendung auf Kriechversuche mit mit französischen und deutschen RDB-Stählen

Reactor Safety Research-project No.: 150 1254
Project Title: Modelling of in-vessel retention after relocation of corium into the lower plenum: evaluation of the temperature field and of the visco-plastic deformation of the vessel wall

Reaktorsicherheitsforschung - Vorhaben Nr.: 150 1254
Vorhabenstitel: Beitrag zur Modellierung der Schmelzerückhaltung im RDB nach Verlagerung von Corium in das untere Plenum: Berechnung des Temperaturfeldes und der visko-plastischen Verformung der Behälterwand

Hinweis:

Das diesem Bericht zugrundeliegende Vorhaben wurde mit Mitteln des Bundesministeriums für Wirtschaft und Technologie unter dem Förderkennzeichen GRS 150 1254 gefördert. Die Verantwortung für den Inhalt dieser Veröffentlichung liegt bei den Autoren.

Abstract

Considering the hypothetical core melt down scenario for a light water reactor (LWR) a possible failure mode of the reactor pressure vessel (RPV) and its failure time has to be investigated for a determination of the loadings on the containment. Numerous experiments have been performed accompanied with material properties evaluation, theoretical, and numerical work /REM 1993/, /THF 1997/, /CHU 1999/.
For pre- and post-test calculations of Lower Head Failure experiments like OLHF or FOREVER it is necessary to model creep and plasticity processes. Therefore a Finite Element Model is developed at the FZR using a numerical approach which avoids the use of a single creep law employing constants derived from the data for a limited stress and temperature range. Instead of this a numerical creep data base (CDB) is developed where the creep strain rate is evaluated in dependence on the current total strain, temperature and equivalent stress. A main task for this approach is the generation and validation of the CDB. Additionally the implementation of all relevant temperature dependent material properties has been performed. For an evaluation of the failure times a damage model according to an approach of Lemaitre is applied.
The validation of the numerical model is performed by the simulation of and comparison with experiments. This is done in 3 levels: starting with the simulation of single uniaxial creep tests, which is considered as a 1D-problem. In the next level so called "tube-failure-experiments" are modeled: the RUPTHER-14 and the "MPA-Meppen"-experiment. These experiments are considered as 2D-problems. Finally the numerical model is applied to scaled 3D-experiments, where the lower head of a PWR is represented in its hemispherical shape, like in the FOREVER-experiments. This report deals with the 1D- and 2D-simulations.
An interesting question to be solved in this frame is the comparability of the French 16MND5 and the German 20MnMoNi55 RPV-steels, which are chemically nearly identical. Since these 2 steels show a similar behavior, it should be allowed on a limited scale to transfer experimental and numerical data from one to the other.

Kurzfassung

Bezüglich eines hypothetischen Kernschmelzeszenarios in einem Leichtwasserreaktor ist es notwendig, mögliche Versagensformen des Reaktordruckbehälters sowie Versagenszeiträume zu untersuchen, um die Belastung für das Containment bestimmen zu können. Es wurden bereits eine Reihe von Experimenten durchgeführt, welche Erkenntnisse hierüber liefern sollen. Begleitend wurden in Einzelversuchen Materialeigenschaften ermittelt, sowie theoretische und numerische Arbeiten durchgeführt.
Für die Simulation von Experimenten zum Versagen der Bodenkalotte, wie OLHF oder FOREVER, ist es notwendig, Kriechen und Plastizität zu berücksichtigen. Hierfür wurde am FZR ein Finite Elemente Model entwickelt, das die Verwendung von einfachen Kriechgesetzen, die mit ihren angepassten Konstanten nur für begrenzte Spannungs- und Temperaturbereiche gültig sind, umgeht. Stattdessen wird eine numerische Kriechdatenbasis angelegt, in der die Kriechdehnrate in Abhängigkeit von der Gesamtdehnung, der Temperatur und der Vergleichsspannung abgelegt ist. Die Hauptaufgabe für diese Vorgehensweise besteht in der Generierung und Validierung der Kriechdatenbasis. Zusätzlich wurden alle relevanten temperaturabhängigen Materialeigenschaften mit entsprechenden Modellen in den Code eingegeben. Für die Bestimmung der Versagenszeit wurde ein Schädigungsmodel nach einem Vorschlag von Lemaitre implementiert.
Die Validierung des numerischen Models erfolgt durch die Simulation von und den Vergleich mit Experimenten. Dies geschieht in 3 Stufen: zunächst werden einzelne einachsige Kriechversuche nachgerechnet, was als 1D-Problem bezeichnet wird. In der nächsten Stufe werden so genannte „Rohrversagensexperimente" simuliert: das RUPTHER-14 und das „MPA-Meppen"-Experiment. Diese Experimnete werden als 2D-Probleme betrachtet. Schließlich kann das Modell auf skalierte 3D-Versuche angewendet werden, in denen die Bodenkalotte eines Druckwasserreaktors mit ihrer halbkugelförmigen Geometrie wiedergegeben wird. Ein Beispiel hierfür sind die FOREVER-Experimente. Dieser Bericht behandelt die 1D- und 2D-Simulationen.
Eine wichtige Frage im Rahmen dieser Arbeit ist die Vergleichbarkeit des französischen Reaktordruckbehälterstahls 16MND5 und des deutschen 20MnMoNi55, welche chemisch nahezu identisch sind. Da diese beiden Stähle ein ähnliches Verhalten zeigen, sollte es in gewissem Umfang zulässig sein, experimentelle und numerische Daten und Erkenntnisse zwischen beiden zu übertragen.

Contents

List of Figures

Nomenclature

Latin Symbols

A	$[m^2]$	area
c_p	[J/kgK]	specific isobaric heat capacity
D	[-]	damage parameter
ΔD	[-]	damage parameter increment
E	[Pa]	Young´s modulus
F	[N]	force
i	[-]	counter
L	[m]	length, distance
R_v	[-]	triaxiality function
T	[°C]; [K]	temperature
ΔT	[K]	temperature difference
t	[s]; [min]; [h]	time
Δt	[s]	time step
V	$[m^3]$	volume

Greek Symbols

α	$[K^{-1}]$	thermal expansion coefficient
ε	[-]	strain
$\dot{\varepsilon}$	$[s^{-1}]$	strain rate
λ	[W/mK]	heat conductivity
ν	[-]	Poisson´s number
ρ	$[kg/m^3]$	density
σ	[Pa]	stress

Indices

0	original, at the beginning
cr	creep
el	elastic
eqv	equivalent
frac	fracture, rupture
h	hydrostatic
inst	instantaneous; current
max	maximal
min	minimal
n	nominal, engineering
pl	plastic
ref	reference
t	true

Abbreviations

CDB	Creep Data Base
CFD	Computational Fluid Dynamics
FE	Finite Element
FOREVER	Failure Of REactor VEssel Retention
LWR	Light Water Reactor
OLHF	OECD Lower Head Failure Program
RPV	Reactor Pressure Vessel
PWR	Pressure Water Reactor
UPF	User Programmable Feature

1. Introduction

The hypothetical scenario of a severe accident with core meltdown and formation of a melt pool in the lower plenum of a Light Water Reactor (LWR) Pressure Vessel (RPV) can result in the failure of the RPV and the discharging of the melt to the containment. One accident management strategy could be to stabilize the in-vessel debris or melt pool configuration in the RPV as one major barrier against uncontrolled release of heat and radionuclides.

To obtain an improved understanding and knowledge of the melt pool convection, the vessel creep, possible failure processes and modes occurring during the late phase of a core melt down accident the FOREVER-experiments (Failure Of REactor VEssel Retention) are currently being performed at the Division of Nuclear Power Safety of the Royal Institute of Technology, Stockholm /SEH 1999/. These experiments are simulating the behavior of the lower head of the RPV under the thermal loads of a convecting melt pool with decay heating, and under the pressure loads that the vessel experiences in a depressurized vessel scenario (cf. Fig. 1). The geometrical scale of the experiments is 1:10 compared to a prototypic LWR. Due to the multi axial creep deformation of the vessel with a non-uniform temperature field these experiments are on the one hand an excellent

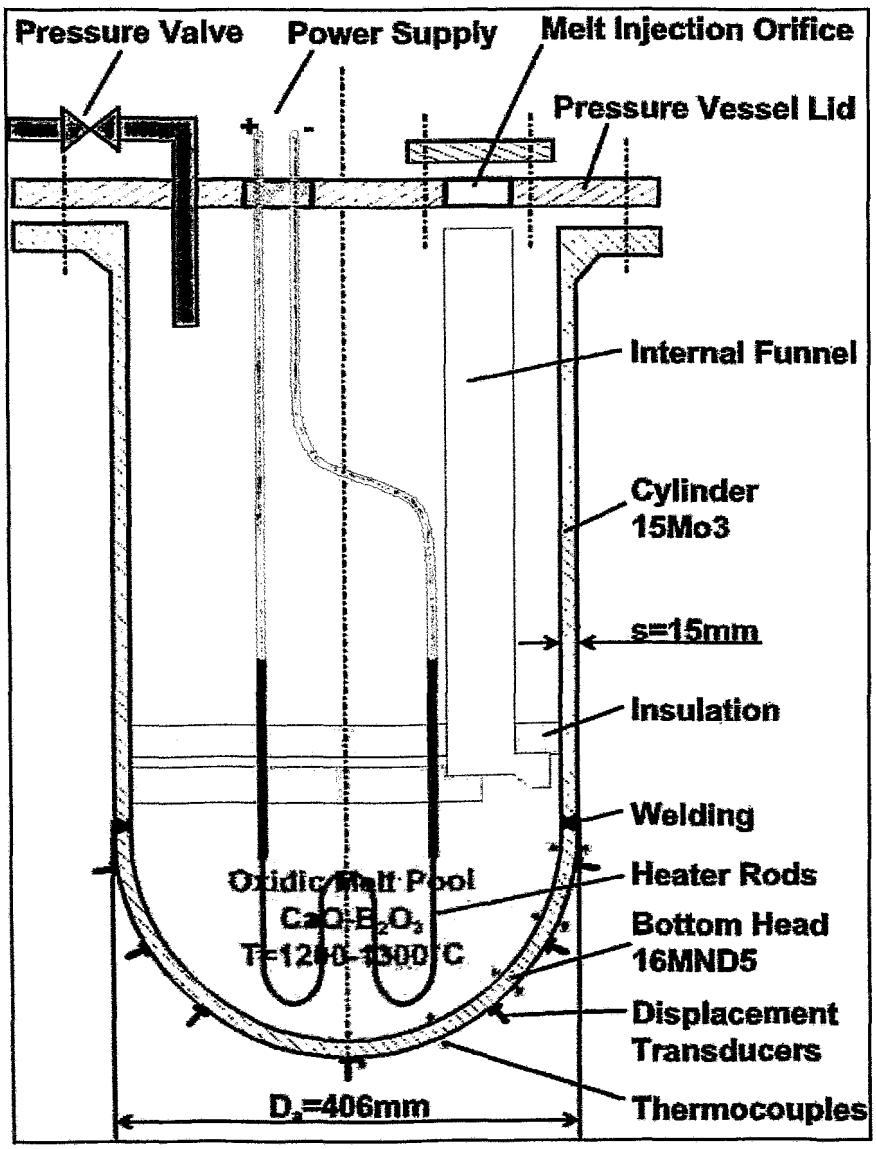

Figure 1: Principal experimental setup of FOREVER - not to scale.

source of data to validate numerical creep and damage models which are developed on the basis of uniaxial creep tests. On the other hand the results of pre-test calculations can be used to optimize the experimental procedure and can help to make on-site decisions during the experiment.
Therefore an axisymmetric Finite Element (FE) model is developed based on the multi-purpose code ANSYS/Multiphysics®. Using the Computational Fluid Dynamics (CFD) module the melt pool convection is simulated and the temperature field within the melt pool and within the vessel wall is calculated. The transient structural mechanical calculations are then performed applying a creep model which takes into account the large temperature, stress and strain variations.
A main task for the numerical creep model approach is the development and validation of the creep data base (CDB). The source for the CDB are uniaxial creep tests, like the REVISA-experiments. The CDB includes the primary, secondary and tertiary creep stages. In the calculation the creep strain rate is then evaluated in dependence on the current total strain, temperature and equivalent stress.
Additionally the implementation of all relevant temperature dependent material properties has been performed. For an evaluation of the failure times a damage model according to an approach of Lemaitre /LEM 1996/ is applied.
The modeling approach and validation is done in 3 steps: starting with the simulation of single uniaxial creep tests, which is considered as a 1D-problem. In the next level so called "tube-failure-experiments" are modeled: the RUPTHER-14 and the "MPA-Meppen"-experiment. These experiments are considered as 2D-problems. Finally the numerical model can be applied to scaled 3D-experiments, where the lower head of a PWR is represented in its hemispherical shape, like in the FOREVER-experiments.
In the frame of this work the comparability of the French 16MND5 and the German 20MnMoNi55 RPV-steel is investigated. If these 2 steels show a similar behavior, it should be allowed to transfer experimental and numerical data in a limited scale from one to the other.

2. Material Properties of the Steel

For the considered tests a precise temperature dependent modeling of all relevant material properties is necessary. Generally the material properties of the French RPV-steel 16MND5 are considered. The material for the 16MND5-specimen, -tubes, or -vessels investigated later was made by Kawasaki Steel, Japan /MON 1999/. Each material property is stored in a table where the temperature ranges from 275 K to 1600 K with 54 equidistant (ΔT=25 K) temperature levels (*MPTEMP-*, *MPDATA-*commands). In the following sections the material data applied in the Finite Element Model is represented.

2.1 Density

Since inertia effects are not important in the considered tests until failure and the simulations stop with failure, the density influences the observed results in some calculations only slightly due to the deadweight of the structure, which depends on the experimental setup.

The temperature dependent density generally decreases from ρ=7850 kg/m^3 at room temperature to ρ=7378 kg/m^3 at 1600 K. During the phase transformation, which is for low carbon steels at low heating rates between A_{C1}=723 °C and A_{C3}=830 °C and which is modeled in the calculation from 1000 K to 1100 K, there is a slight density

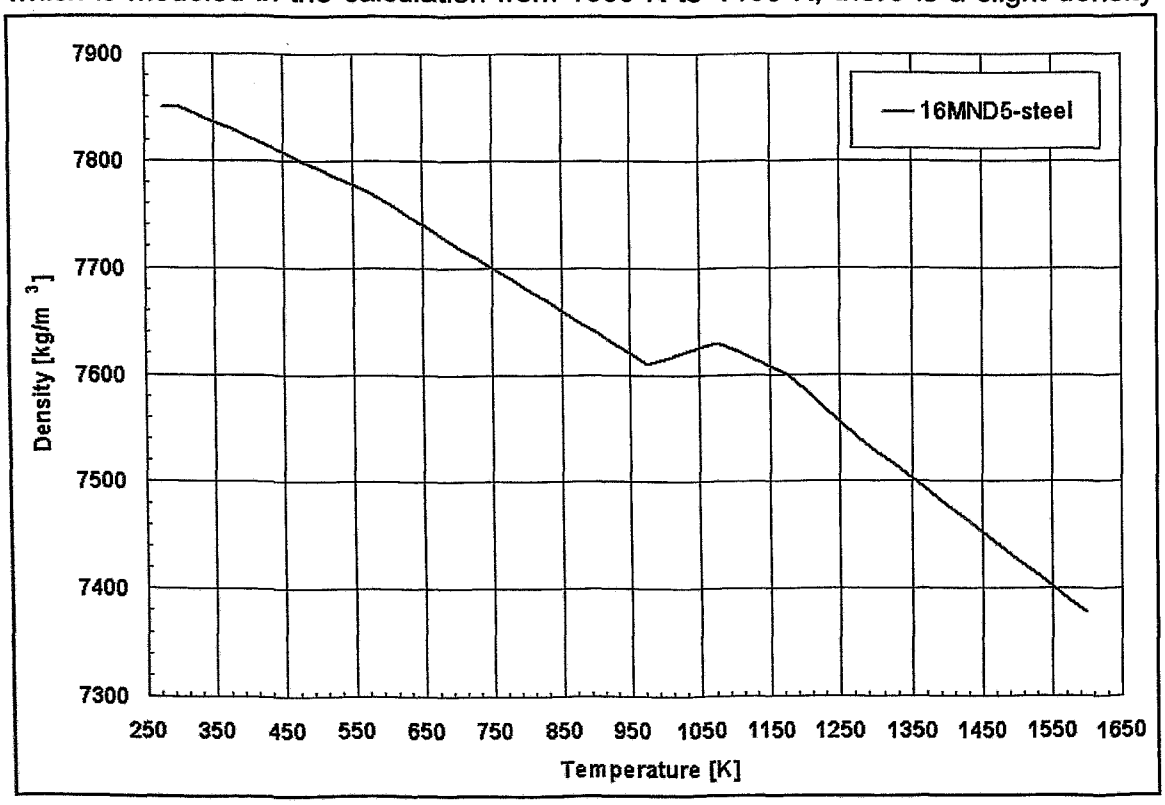

Figure 2: Temperature dependent density.

increase with increasing temperature, i.e. the structure is shrinking.

2.2 Thermal Expansion Coefficient

The thermal expansion coefficient is relevant for the simulation of structures with temperature differences and/or transient temperatures during loading. The mean thermal expansion coefficient $\alpha(T)$ shown in Fig. 3 is the average of the instantaneous expansion coefficient $\alpha_{inst}(T)$ from the reference temperature to the actual temperature. The relation is represented in the following equation:

$$\alpha(T) = \frac{\int_{T_{ref}}^{T} \alpha_{inst}(T)\, dT}{T - T_{ref}} \qquad \text{Eq. 1}$$

I.e., during the phase transformation between 1000 K to 1100 K the mean expansion coefficient just decreases, while the instantaneous expansion coefficient is negative. During the heat up or cool down of a structure the different expansion behavior inside and outside of the phase transformation can cause additional thermal stress especially if there are large temperature differences within the structure.

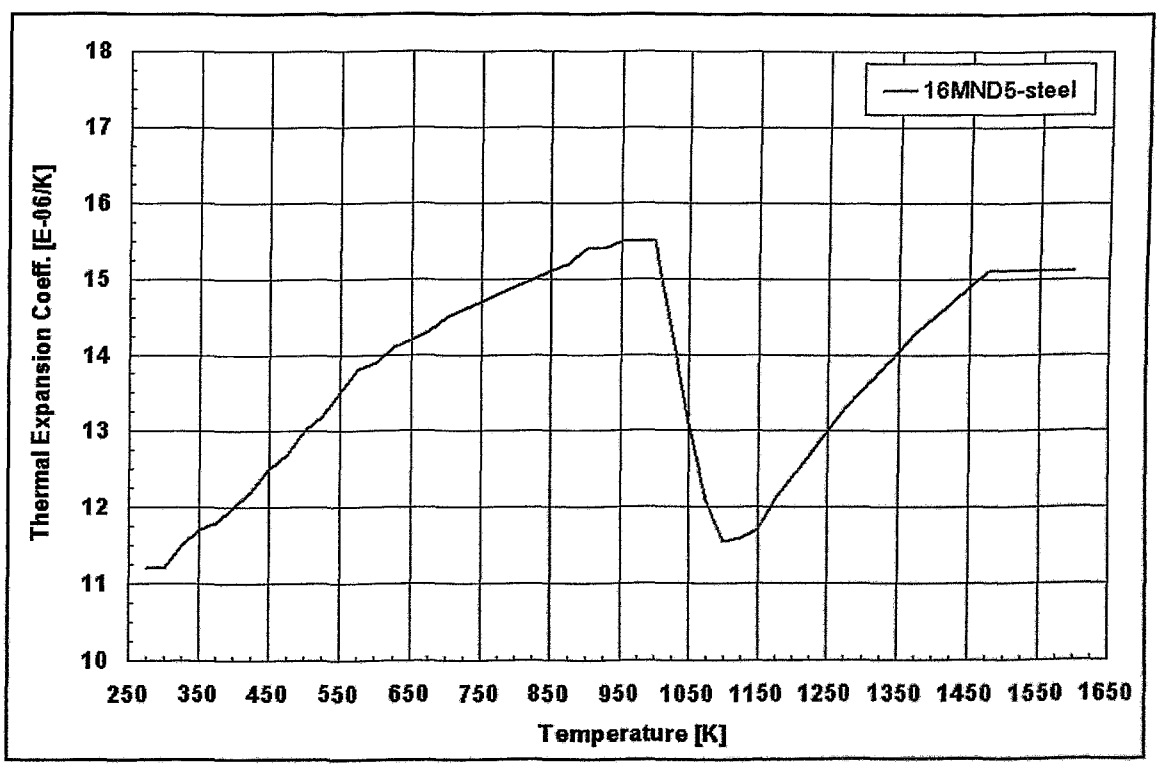

Figure 3: Temperature dependent mean thermal expansion coefficient.

2.3 Thermal conductivity

The temperature dependent thermal conductivity is required if there are heat fluxes through the considered structure and the temperature field is evaluated by a thermal calculation prior to the mechanical calculation.

As typical for ferritic/bainitic low alloy steels the conductivity is around λ=40 W/mK for low temperatures and decreases to 25 to 30 W/mK at high temperatures.

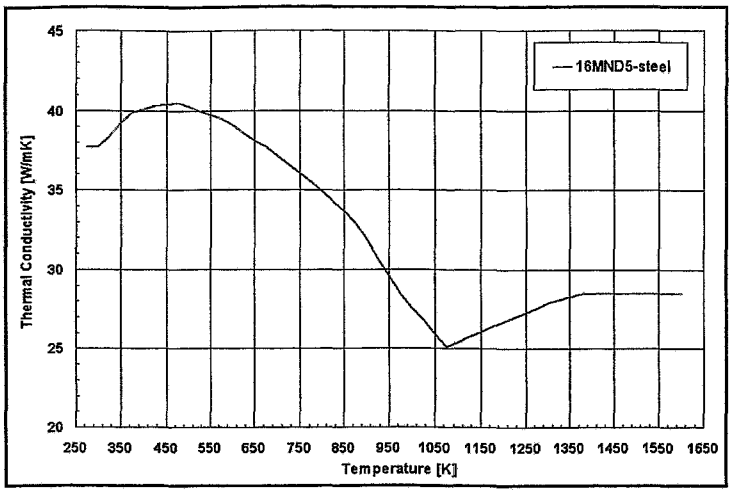

Figure 4: Temperature dependent thermal conductivity.

2.4 Heat capacity

The consideration of the temperature dependent heat capacity is necessary for scenarios with transient temperature fields.

The capacity increases from some c_p=500 J/kgK at room temperature to 800 J/kg at the beginning of the phase transformation. During the phase transformation the heat capacity reaches values of 1400 J/kgK and after that it is around 600 J/kgK. The latent heat of fusion for the melting process is not modeled because the melting point is above the considered temperature range.

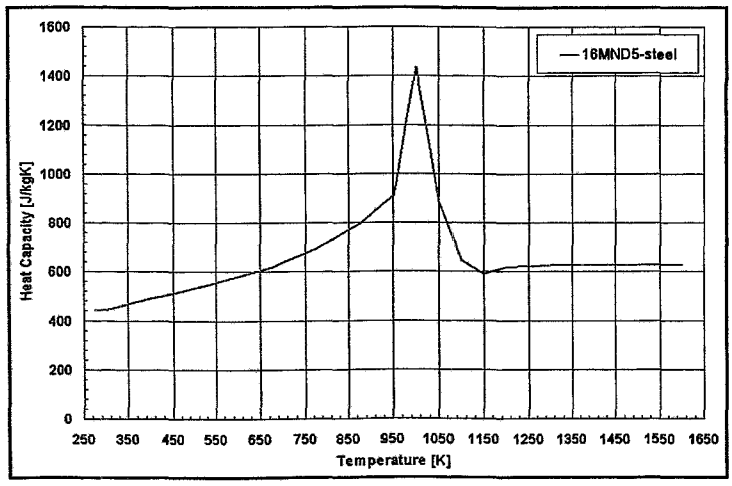

Figure 5: Temperature dependent heat capacity.

2.5 Young's Modulus

The temperature dependent behavior of the Young´s modulus is shown in Figure 6. For comparison the Young´s modulus is plotted to the right axis and the yield stress and the true ultimate stress are plotted to the left axis. The Young´s modulus starts at room temperature with E=199 GPa. All properties are declining with increasing temperature, but have the steepest decline around 900 K.

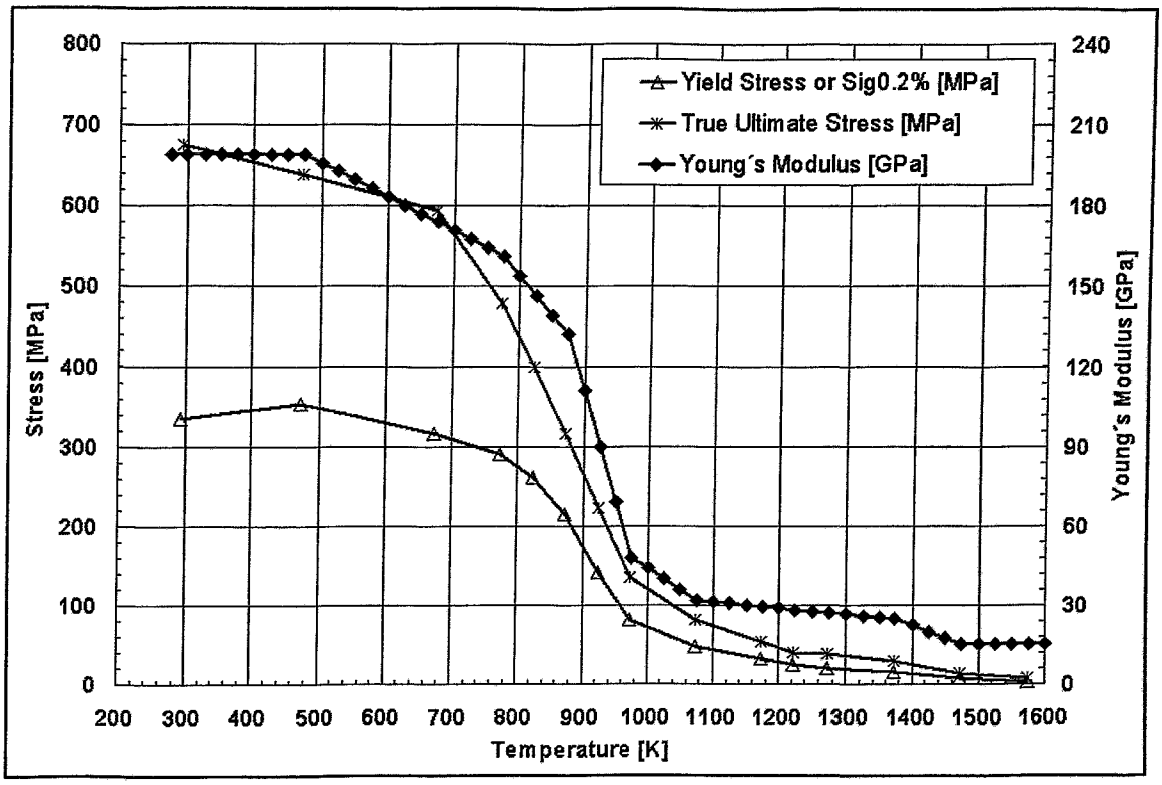

Figure 6: Temperature dependent Young's Modulus and yield stress and true ultimate stress as measured in tensile tests.

2.6 Plasticity

Additionally to the creep model described later a plasticity model is used to be able to model prompt failure. In addition to creep, which is time dependent, it is necessary to model plasticity, which takes place instantaneously. In fact, both phenomena can not be distinguished clearly in all cases, but to be conservative for all scenarios both deformation and failure criteria are included.

For the plasticity the multilinear isotropic hardening model of the ANSYS code is used (*MISO*-option). For 12 temperature levels from room temperature to 1600 K the plasticity is represented by a curve consisting of 5 linear sections. The strain given in the curve is the total strain, including elastic strain, but no thermal strain.. For an overview Figure 18 in the appendix presents the engineering stress-strain curves of all REVISA tensile tests.

As an example Figure 7 represents the relations at 800 °C. The dotted black curve shows the modeled stress-strain relation of the code. The plasticity in the FE model is a prompt plasticity, i.e. if the stress reaches a certain value at a time the corresponding strain is modeled instantly. Contrary to this the tensile tests in the REVISA program were performed at a constant nominal or engineering strain rate of $\dot{\varepsilon}$=1 %/min for tests below 1000 °C (test specimen length: 50 mm, displacement

rate: 0.5 mm/min) and 1.176 % for 1000 °C and higher (test specimen length: 85 mm, displacement rate: 1.0 mm/min). The following explanations are oriented to uniaxial tensile tests with cylindrical test specimen.
The blue curve in Figure 7 shows the measured values of the engineering or nominal stress-strain relation. The engineering / nominal stress is defined as:

$$\sigma_n(t) = \frac{F(t)}{A_0} \qquad \textbf{Eq. 2}$$

Where F(t) is the current measured force and A_0 the original cross sectional area. And the engineering strain is calculated by:

$$\varepsilon_n = \frac{L(t) - L_0}{L_0} \qquad \textbf{Eq. 3}$$

With L(t) and L_0 as the current and original length of the specimen, respectively. For small strains the accuracy of these engineering values is sufficient, but for large deformation analysis the natural strain and the true stress are needed. The natural or true strain increment is defined as:

$$d\varepsilon_t = \frac{dL}{L} \qquad \textbf{Eq. 4}$$

The integration from the original length L_0, where $\varepsilon=0$, to the actual length L(t) provides the true strain:

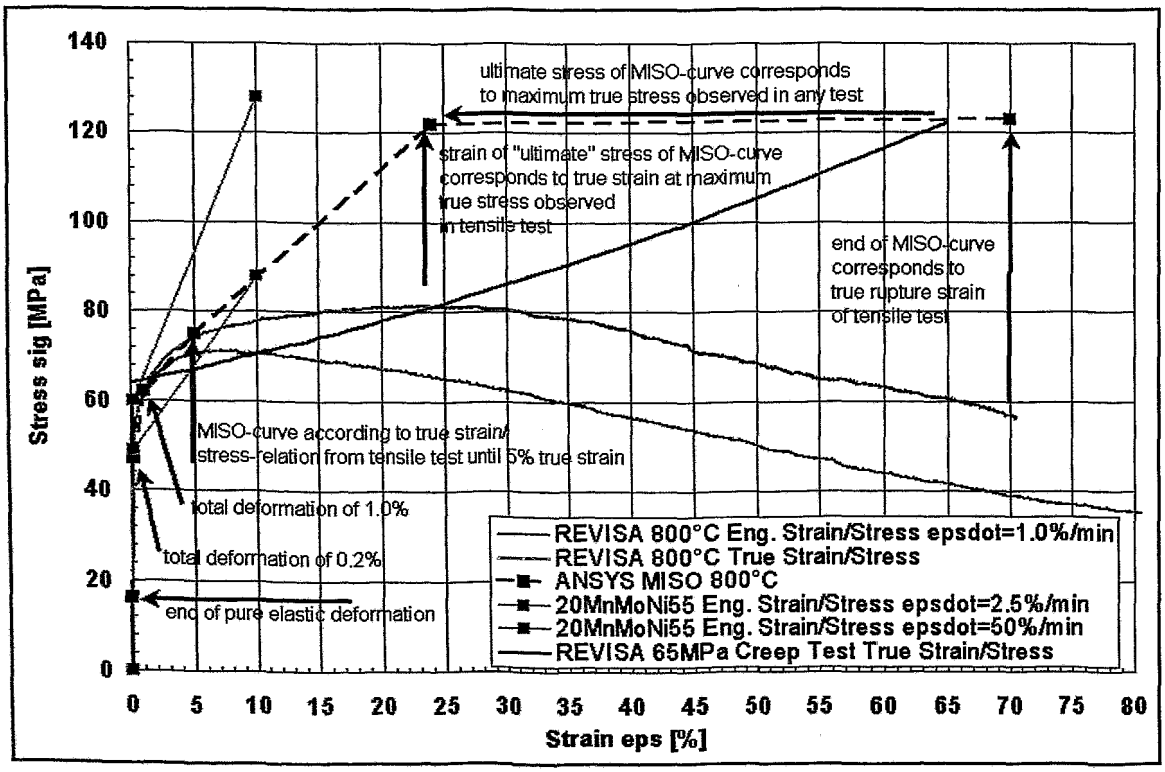

Figure 7: Plasticity curves and model at 800°C.

$$\varepsilon_t = \int_{L_0}^{L(t)} \frac{dL}{L} = \ln\frac{L(t)}{L_0} = \ln\left(1+\frac{L(t)-L_0}{L_0}\right) = \ln(1+\varepsilon_n) \qquad \textbf{Eq. 5}$$

To get the true stress the instantaneous cross sectional area A(t) has to be considered:

$$\sigma_t(t) = \frac{F(t)}{A(t)} \qquad \textbf{Eq. 6}$$

Usually the volume change due to plasticity or creep is negligible, i.e., the volume at any time during the plasticity or creep process is constant (except for tertiary creep, which is not considered here) after unloading the structure, so that there is no elastic volume change. This means, that the original volume V_0 of the unloaded structure is the actual volume V(t) subtracted by the elastic volume change V_{el}:

$$V_0 = V(t) - V_{el}(t) = A_0 \cdot L_0 \qquad \textbf{Eq. 7}$$

For the elastic volume change following relation applies:

$$V_{el} = L_0(1+\varepsilon_{el}) \cdot A_0(1-\nu\cdot\varepsilon_{el})^2 - L_0 \cdot A_0 \qquad \textbf{Eq. 8}$$

Usually the elastic strain is rather small (<0.5 %, cf. Figure 6), also for large total strains. Therefore the elastic volume change can be neglected and equation 7 reduces to:

$$V_0 = A_0 \cdot L_0 \approx A(t) \cdot L(t) \qquad \textbf{Eq. 9}$$

Using equations 6, 9 and 3 the true stress becomes:

$$\sigma_t(t) = \frac{L(t)}{L_0} \cdot \frac{F(t)}{A_0} = (1+\varepsilon_n) \cdot \sigma_n \qquad \textbf{Eq. 10}$$

And finally using eq. 5 the true stress is defined as:

$$\sigma_t(t) = e^{\varepsilon_t} \cdot \sigma_n \qquad \textbf{Eq. 11}$$

Plotting the true stress against the true strain gives the red curve in Figure 7 (cf. also Figure 19 in the appendix). It is visible that the true stress is higher than the engineering stress at the same strain. At the maximum of the true curve the start of necking can be assumed. I.e., the true stress at the smallest cross area is higher than the calculated true stress with an assumed homogeneous deformation of the specimen. On the other hand the true rupture strain is smaller than the engineering rupture strain. But both figures of the true curve - stress and strain - are assumed as conservative.

During the post-test calculations of all REVISA creep tests /SAI 1998/ it was observed that the conservative theoretical true stress calculated for the experimental measurement according to equation 11 at the end of the highest load creep tests can be clearly higher than the values from the tensile tests. For the 800°C level this is shown in Figure 7 by the continuous black curve (REVISA 65MPa Creep Test) which

reaches a true stress value of more than 120 MPa contrary to only some 80 MPa in the tensile test.
The reason is the deformation velocity: at high deformation velocities the resistance of the material is higher than at low deformation velocities. This can be seen from experimental results for the German 20MnMoNi55 steel, which is assumed to be similar to the French 16MND5 as explained later.
The 800 °C tensile tests for the German steel were performed at 2 different strain rates: 2.5 %/min and 50 %/min. The measured values for the engineering yield stress and the ultimate stress are given in Figure 7. Since the strain rate of the RE-VISA tensile tests was even lower (1 %) lower corresponding stresses can be expected here. Even considering the fact of 2 similar but still different steels the relation of the strain rate velocity and the corresponding ultimate stress is reasonable. The conclusion is, that at the lower strain rate the deformation is not a pure plastic one since plasticity and creep can occur simultaneously.
Finally the multilinear isotropic hardening curve in the code (MISO-option of ANSYS) has the following structure:

- Pure elastic deformation until 0.05 % strain.
- Stress at 0.2 % plastic strain according to true measurement curve.
- Stress at 1.0 % plastic strain according to true measurement curve.
- Stress at 5.0 % plastic strain according to true measurement curve.
- Highest observed tensile or creep test stress at the true strain where the maximum true stress was observed in the tensile test (cf. inscription in Figure 7).

- Approximately 2 % higher stress than previous stress at rupture strain of true strain curve of tensile test (cf. inscription in Figure 7).

This is a reasonable model to take into account prompt plasticity during creep tests of different geometry, temperature and loading history.
The corresponding figures of the other temperature levels are shown in the appendix (Figure 20 to Figure 30).

3. Creep and Damage Modeling in the Transient Mechanical Calculations

Because of the large spatial and transient temperature and stress changes within the vessel wall of a 3D-experiment like FOREVER, an advanced approach for the numerical creep modeling has been developed. Usually creep is described by analytical formulas (creep laws) with a number of free coefficients. The coefficients are used to adapt the creep laws to creep test results performed at constant load and temperature. However, it is difficult to achieve a satisfying adjustment for a wide range of temperatures and stresses with only one set of coefficients. Therefore a supplementary tool for the ANSYS® code has been developed, which allows to describe the creep behavior of a material for different stress and temperature levels independently by means of a creep data base (CDB). The Digital® Fortran Compiler (Rev. 6.5) was used for programming and for generating the customized ANSYS-executable on a Windows/NT® platform (/ALT 2000/, /WIL 2001/). The creep data base has been generated based on an analysis of the measured data performed by Ikonen /IKO 1999/. Due to the uncertainties of the creep fracture strains measured in the uniaxial tests the creep fracture strain ε_{frac}^{cr} was set conservatively for each temperature level. It is ranging from 35% at 600 °C to 65% at 1000 °C. The plasticity of the material is modeled by using the multilinear isotropic hardening option of ANSYS® /ANS 2001/. The plastic fracture strain ε_{frac}^{pl} is evaluated from the last point of the stress-strain curve (cf. chapter 2.6).
For the prediction of a failure time it is necessary to calculate a damage criterion. The material damage due to significant creep and plastic strains is modeled by a damage measure D which is incrementally accumulated at the end of a time step or substep. D=0 means "no damage", which is the initial value for all elements. The damage includes also the prompt plastic deformation of the structure. The damage increment is:

$$\Delta D = \left[\frac{\Delta \varepsilon_{eqv}^{cr}}{\varepsilon_{frac}^{cr}(\sigma, T)} + \frac{\Delta \varepsilon_{eqv}^{pl}}{\varepsilon_{frac}^{pl}(T)} \right] \cdot R_v \qquad \text{Eq. 12}$$

with ε_{frac}^{cr} being the creep fracture strain of the uniaxial creep test at constant stress and temperature and ε_{frac}^{pl} being the plastic fracture strain at the corresponding temperature. Both strain components are calculated separately according to the experimentally found material behavior /SAI 1998/, which is described in the next sections. R_v is a function which considers the damage behavior in dependence on the triaxiality of the stress tensor /LEM 1996/:

$$R_v = \frac{2}{3} \cdot (1+\nu) + 3 \cdot (1-2\nu) \cdot \left(\frac{\sigma_h}{\sigma_{eqv}} \right)^2 \qquad \text{Eq. 13}$$

where ν is the elastic Poisson's ratio, σ_h is the hydrostatic stress and σ_{eqv} is the von-Mises equivalent stress. The damage increment is calculated for each element by averaging its nodal equivalent creep strains. The accumulated damage is:

$$D = \sum_{i=1}^{ldstep} \Delta D_i \qquad \text{Eq. 14}$$

If the element damage reaches the value of D=1, the element is killed by setting its death flag to 1, i.e., this element does no longer contribute to the wall strength. The implementation of this model is described in /ALT 2000/.

4. The Considered French 16MND5 and German 20MnMoNi55 Steels

In this work 2 nominal types of RPV-steel are considered in different tests: the French 16MND5 and the German 20MnMoNi55. At first the Creep Data Base (CDB) is developed from uniaxial creep tests (/SAI 1998/ and /IKO 1999/) of the French 16MND5 RPV-steel and then the comparability of the 2 steels is investigated.
Figure 8 shows the region that is covered by the CDB. The arrays 1 to 4 show the points where uniaxial creep test were performed. The upper bound is not only depended from the true ultimate stress of the corresponding tensile test, but also from the maximum observed theoretical true stress of any creep test at the corresponding temperature (cf. chapter 2.6 Plasticity).
There are 8 temperature levels in the CDB starting from 873 K up to 1573 K in steps of 100 K. At each temperature level there are 5 equidistant stress levels ranging from 20 % of the yield stress of the next higher temperature level to the ultimate stress level of the next lower temperature level. I.e. the numerical CDB provides also temperature and stress combinations where the stress is higher than the ultimate stress which is physically unrealistic. However, these areas of the CDB are never used because the plasticity model of ANSYS causes a failure after reaching the ultimate stress (cf. chapter 2.6 Plasticity).

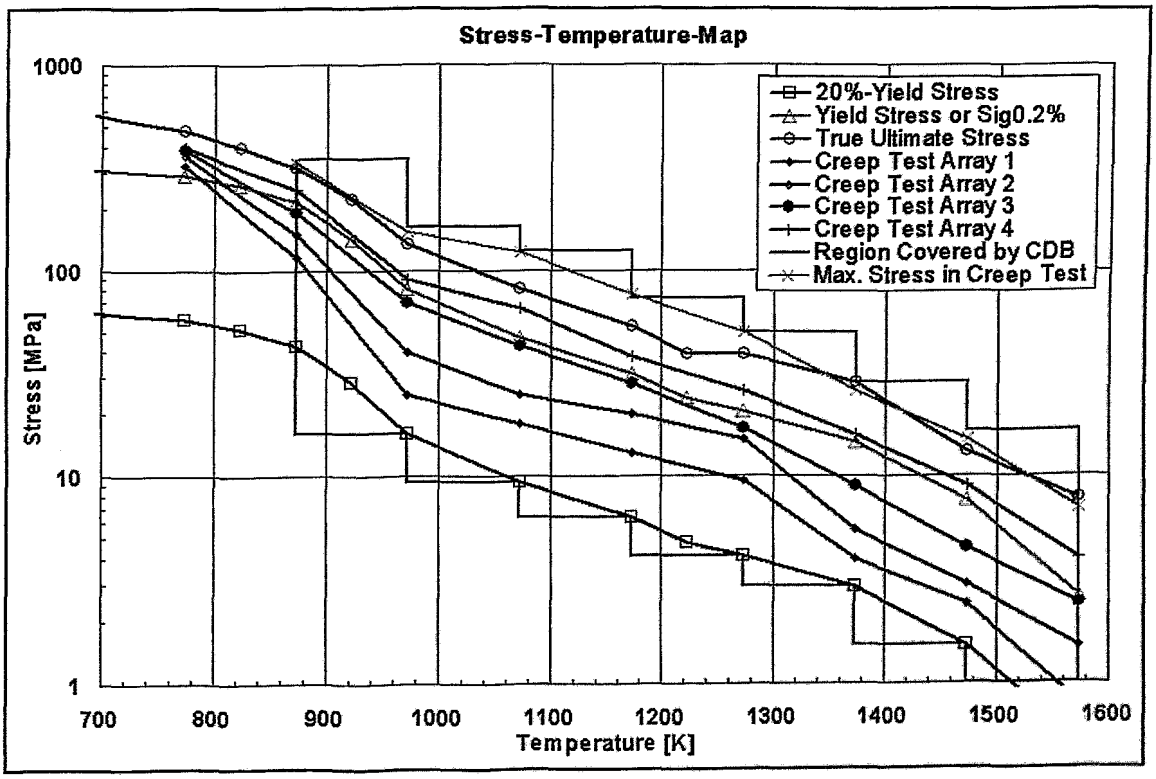

Figure 8: Stress-temperature range covered by the 16MND5-based CDB.

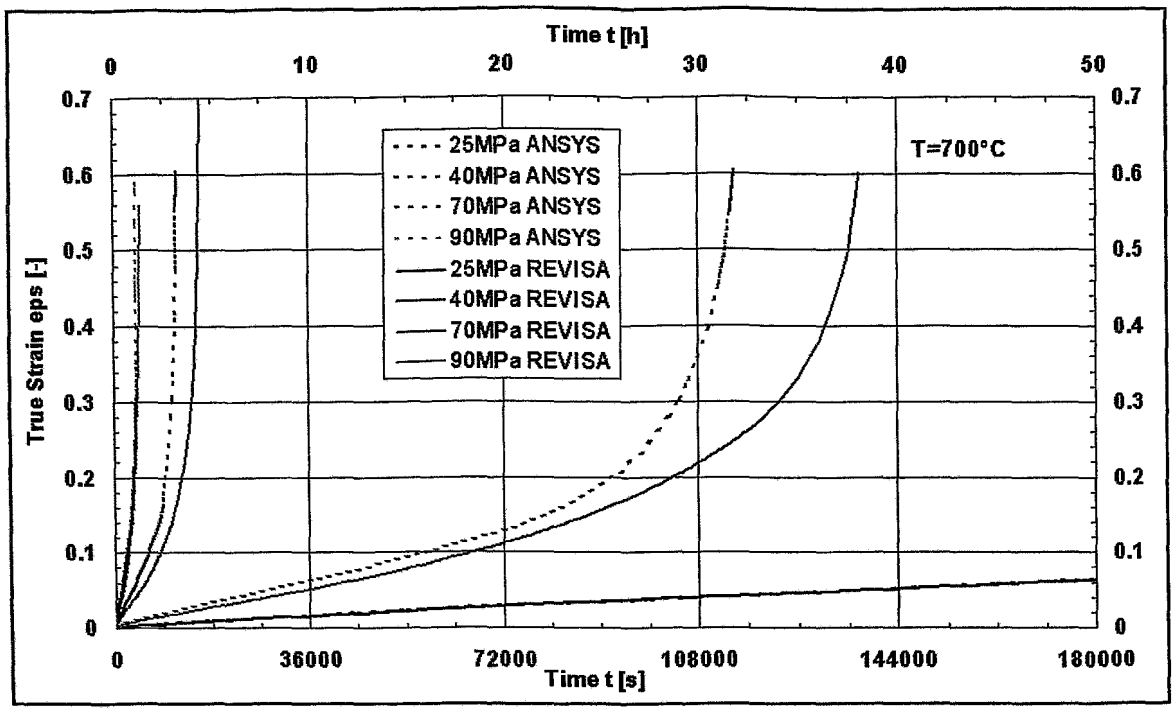

Figure 9: Comparison of uniaxial creep tests at 700°C.

As an example Figure 9 shows the comparison of the REVISA tests at 700 °C with the calculated results from ANSYS. There are some deviations between the calculated and experimental results, but they are considered as acceptable in view of:

i) only small conservative deviations of less than 20 % for the short time runs (like the 90 and 70 MPa-runs) and

ii) a conservative behavior for long time runs (like the 40 MPa-run).

The reason is that the main application of this CDB is related to experiments and prototypic scenarios where a short to medium failure time range is investigated or expected, i.e. typically between 1 and 20 hours. On the other hand it is not known whether each experimental creep curve is really representative, because there is a large scatter even for different specimen of the same heat when tested at the same temperature and stress level.

This can be seen in Figure 10, which shows uniaxial creep tests for the French and the German steel at 800°C and an engineering stress of 65MPa. There was only 1 test of 16MND5 (CEA), whereas there were 5 tests of 20MnMoNi55 (MPA) with the fastest and the slowest creep curve shown. The failure occurred after 4,700s in the slowest test and after 3,800s in the fastest test. This corresponds to a difference of some 20%, and gives an idea about the scatter that can be expected for the 16MND5 tests, too. Finally, the red curve shows the calculated ANSYS curve corresponding to the developed 16MND5-based CDB.

The comparison of all REVISA creep tests from 600°C to 1300°C is shown in the appendix (Figure 31 to Figure 37).

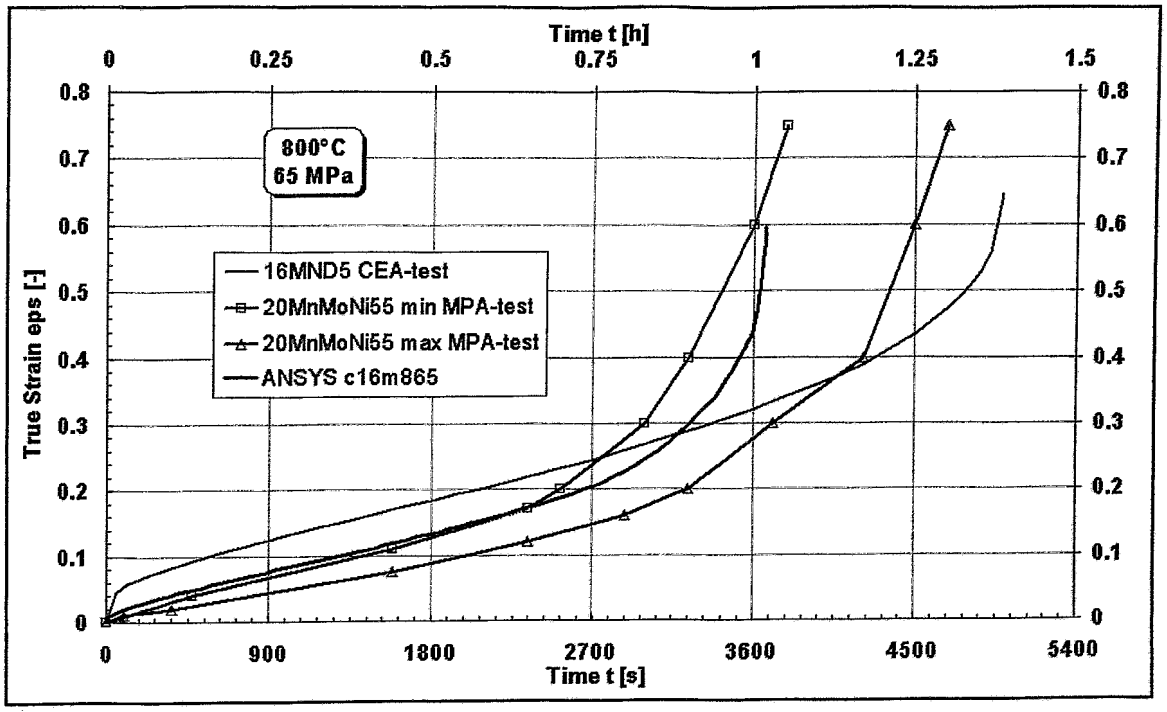

Figure 10: Comparison of the creep behavior of 16MND5 and 20MnMoNi55 with the applied ANSYS CDB at 800°C and 65MPa.

Table 1 lists the chemical composition, the thermal treatment, and the mechanical properties at room temperature of the considered steels. Comparing the chemical composition it seems that the differences between the two 16MND5 heats are in the same range as the differences of the 16MND5 steel to the 20MnMoNi55 steel. Also the thermal treatment seems to be rather similar. The assumption of similarity is supported by the resulting bainitic microstructure of all specimen.
There are some differences in the mechanical properties, but even the weaker 16MND5 values for the yield and tensile strength would fulfill the regulation values according to the German KTA 3201.1.
After analyzing these figures it is assumed that an application of the 16MND5-based CDB to creep tests with 20MnMoNi55-steel is reasonable.

		16MND5 RUPTHER 14	16MND5 FOREVER EC	20MnMoNi55 MPA-Meppen
Chemical composition	Source:	/MON 1999/	/IMA 2001/	/OBS 1988/
[wt.-%]	C	0.17	0.105	0.21
	Si	0.25	0.241	0.24
	Mn	1.44	1.26	1.48
	P	0.004	0.0017	0.008
	S	0.002	0.0006	0.005
	Cr	0.2	0.249	0.2
	Ni	0.75	0.581	0.8
	Mo	0.51	0.568	0.52
	V	0.004	n/a	0.02
	Cu	0.01	0.115	0.07
	Al	0.016	0.0379	0.015
	Sn	0.001	n/a	0.005
	As	0.001	n/a	0.02
Thermal treatment: A.C.: Air Cooled W.C.: Water Cooled F.C.: Furnace Cooled	Quenching	877~891 °C - 8.7 h/W.C.		920 °C - 6.5 h/W.C.
	Tempering	635~652 °C - 9.0 h/A.C.		655~660 °C - 8.0 h/A.C.
	Simulated Stress Relieving	618~625 °C - 6.3 h/F.C.		n/a
Resulting microstructure:		bainitic	bainitic	bainitic
Mechanical Properties at room temperature:	Yield strength	473-488 MPa		567-624 MPa required: >430 MPa
	Tensile strength	620-724 MPa		635-726 MPa req.: 570-710 MPa
	Elongation	25 %		22 %
	Reduction of area	73 %		64-69 %

Table 1: Comparison of properties and manufacturing data of the investigated steels.

5. RUPTHER post test calculation

The considered RUPTHER-14-experiment was performed at CEA, France /MON 1999/. Figure 11 shows the principal configuration of this tube failure experiment. The test pipe of 16MND5 was 270 mm long and 88.9 mm in diameter. The wall thickness was 2 mm. Due to the centered external heating coil the resulting vertical temperature profile had its maximum in the vertical center, too. Therefore the maximum displacement and the failure can be expected at the vertical center as shown in Figure 12.

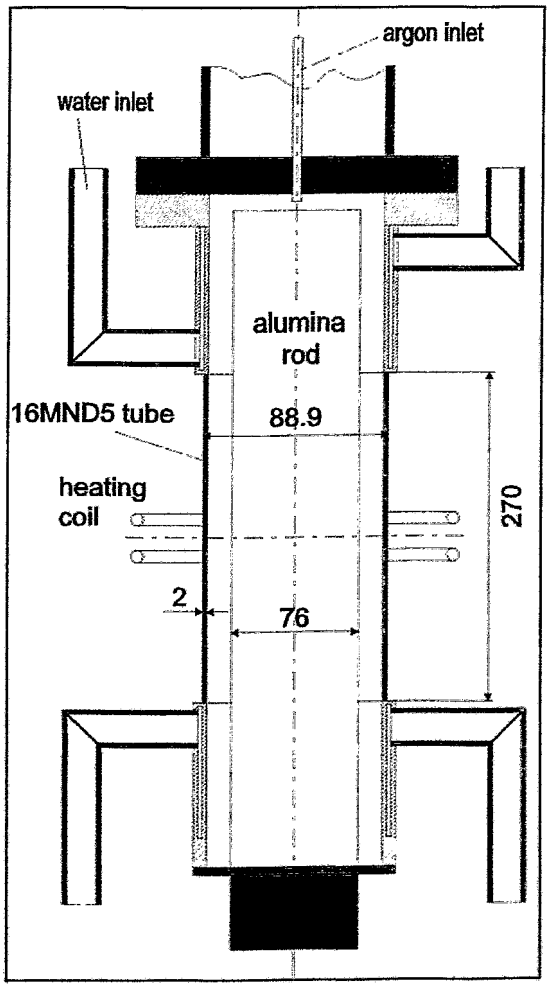

Figure 11: Principal configuration of the RUPTHER-14 experiment [mm].

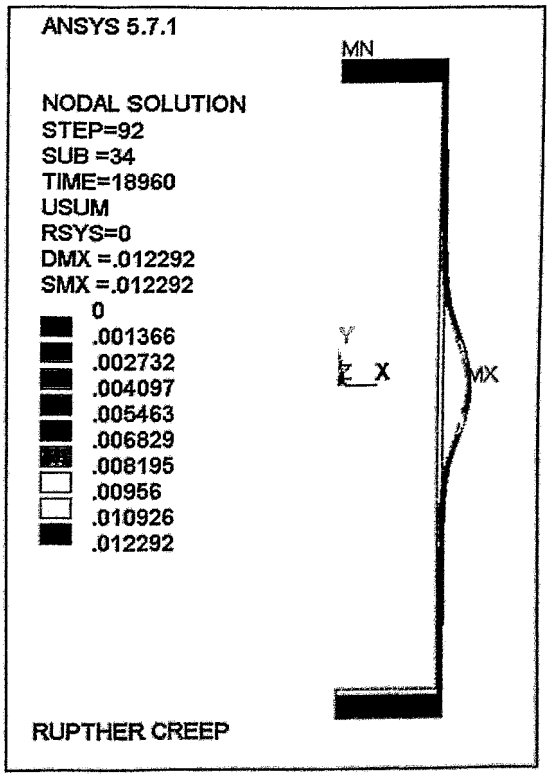

Figure 12: Example of resulting ANSYS deformation at failure [m].

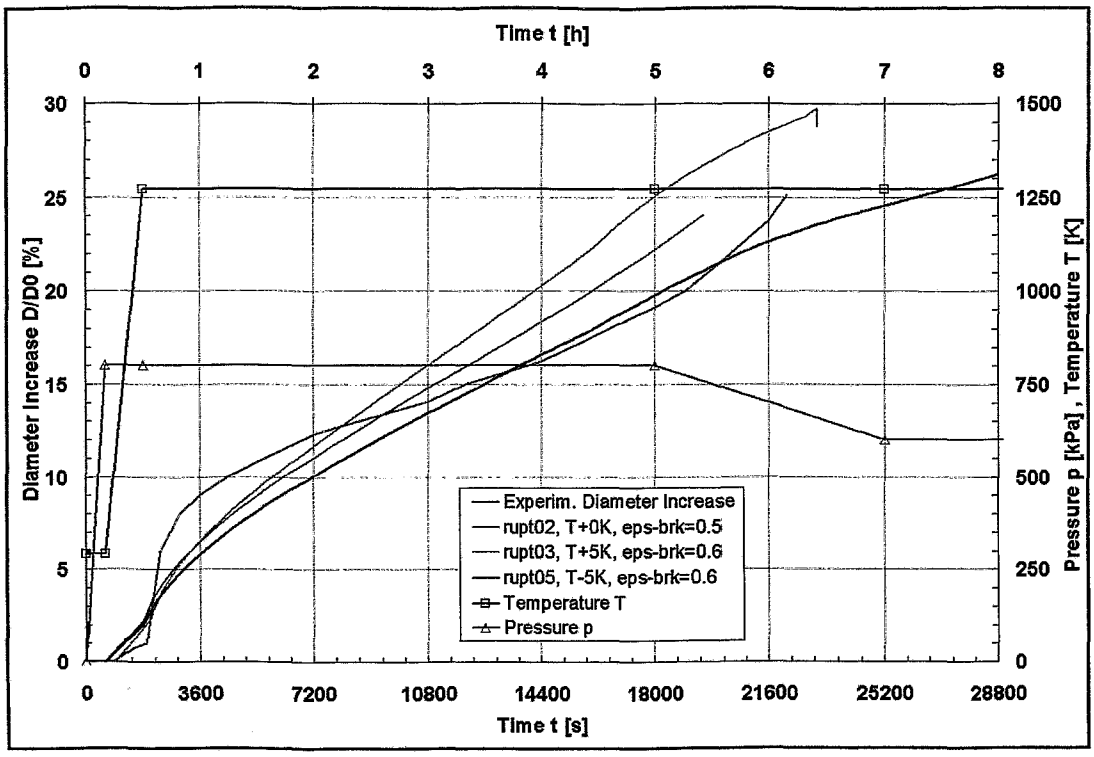

Figure 13: Loading history of RUPTHER-14 and comparison of the measured and calculated diameter increase.

Figure 13 contains the loading history and the central diameter increase of the RUPTHER-14 experiment. After increasing the pressure to 8 bar the temperature was increased to 1000 °C at the hot spot. This regime was kept until 18,000 s, when the pressure was slightly reduced to reach a level of 6 bar after 25,200 s. But the tube failed earlier: at 22,180 s.

Despite of the application of different boundary conditions and slight temperature changes it was not possible to get numerical results for the time dependent diameter increase showing exactly the same behavior as measured. The calculations rupt02 to 05 differ in the slightly changed temperature (+5 K, -5 K respectively) and the assumed rupture strain in rupt02 was reduced to 50 %, while it was normally 60 %. Especially the strong radius increase just after reaching the high temperature level at 1,800 s and the accelerated creep at the pressure reduction stage can not be represented by the code.

If the reason for this discrepancy is not the numerical model, one experimental uncertainty might be the temperature. The temperatures might have been higher in the wall - especially at the beginning of the high temperature level - than the thermocouples show, because they are mounted on the wall. Additionally a distance change between the tube and the induction coil can cause a temperature change. This could be considered for the last stage, when the pressure was dropping, but the creep process accelerated. Another reason can be the scale of the experiment. A wall thickness of 2 mm is relatively thin and small deviations from the design state – either geometrical or material – have a large influence. The suspension effect of relatively thick components does not apply to this thin tube.

6. MPA-Meppen post test calculation

The considered MPA-Meppen test was performed at a test site of the German army in Meppen, Germany /OBS 1988/. Figure 14 shows the principal configuration of this tube failure experiment. The vertically positioned test pipe of 20MnMoNi55 was 2,700 mm long and had an internal diameter of 700 mm. The wall thickness was 47 mm. Several external heating coils were placed vertically around the pipe and the resulting vertical temperature profile had its maximum in the vertical center with a measured maximum at the end of the test of 735 °C.
Therefore the maximum displacement and the failure site can be expected at the vertical centre as shown in Figure 15, which shows the upper half of the deformed FE-model. The loading history of the MPA-Meppen test is given in Figure 16. Starting with a pressure of 120 bar, the pressure was increased to 165 bar and the temperature was increased in three stages to 735 °C at the hot spot. This regime was kept until failure. Because temperatures around 700 °C were only achieved during the last 1,200 s significant deformation is also only recorded for this period. Figure 17shows the comparison of the radius development between the test and different calculations for the last stage. The calculations UR1 to UR3 differ only in their temperature field, which has been shifted by ΔT=5 K up or down.

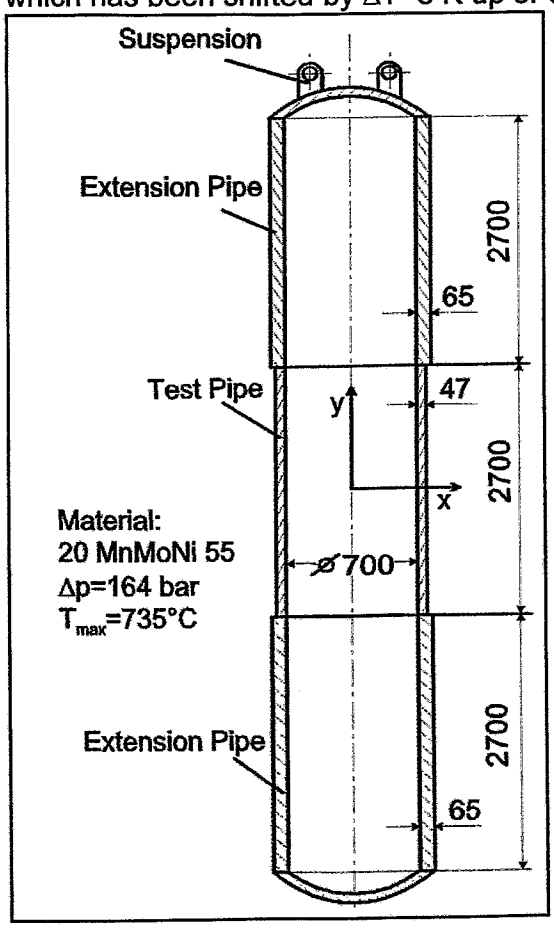

Figure 14: Principal scheme of the MPA-Meppen test [mm].

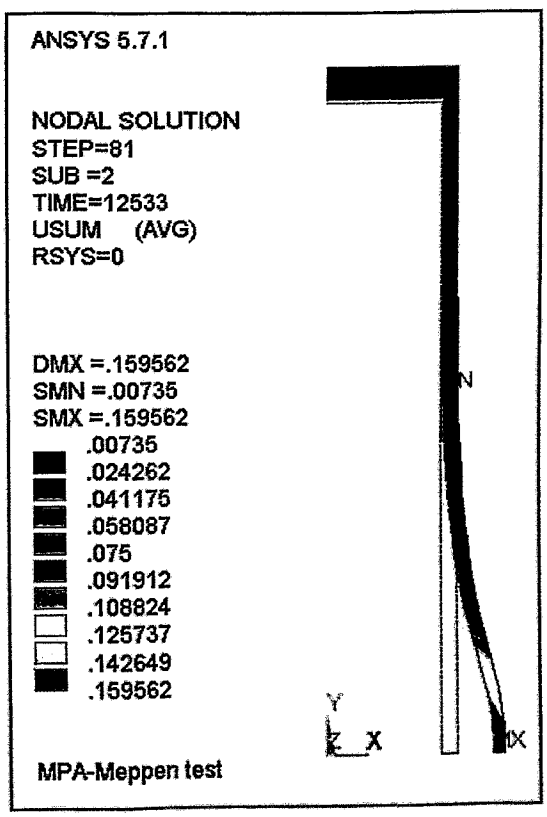

Figure 15: Calculated displacement at failure [m]. (Tmax=998K)

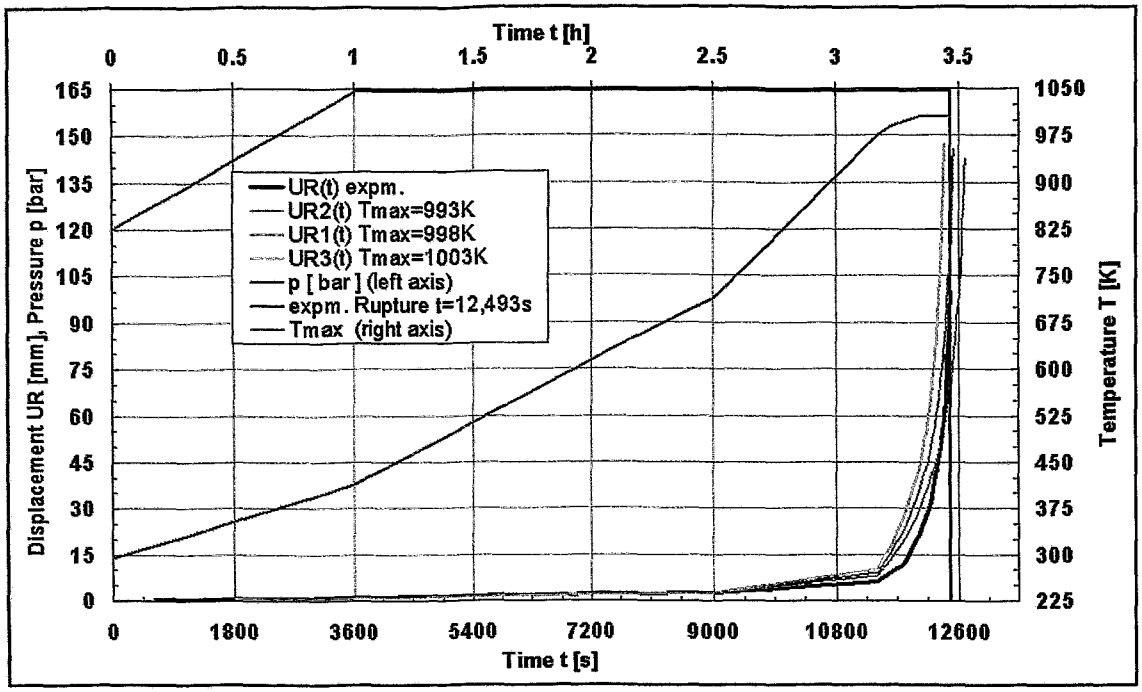

Figure 16: Loading history of MPA-Meppen test and comparison of the measured and calculated radius increase.

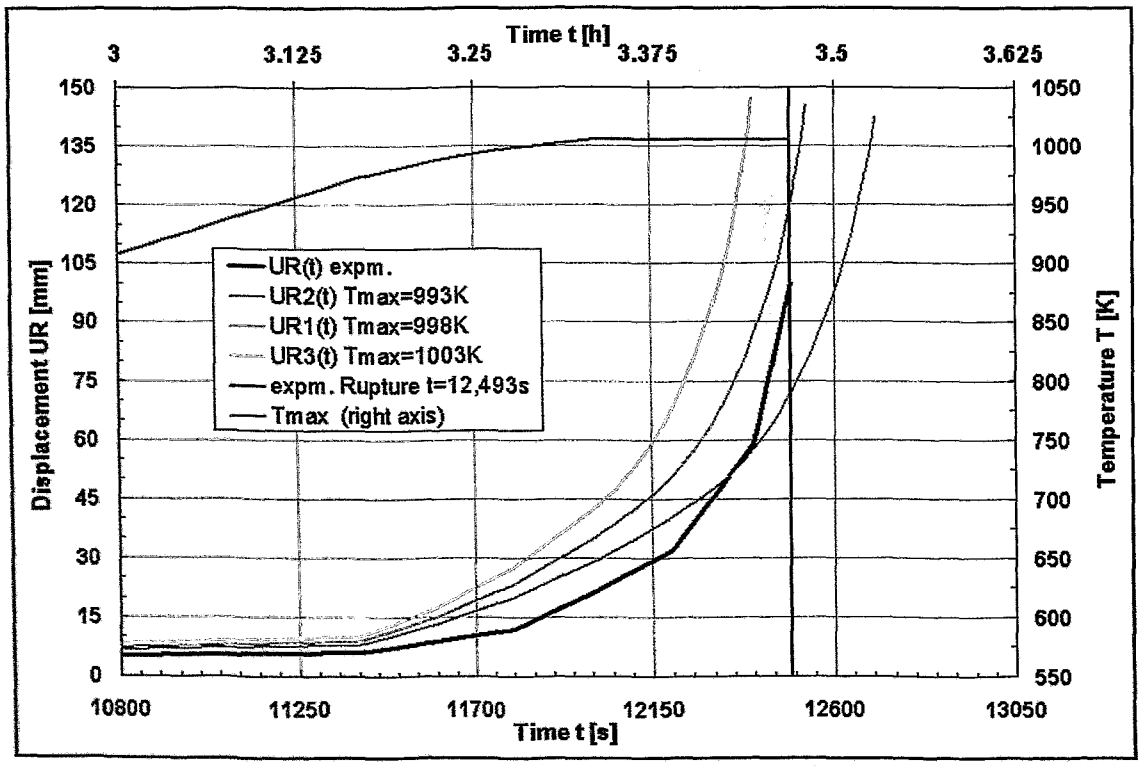

Figure 17: Comparison of the radius development during the last stage of the MPA-Meppen test.

A relatively good agreement between calculation and measurement was achieved. Again a main uncertainty might be the temperature. It is difficult to read and analyse the temperatures from the found literature /OBS 1988/ and additionally there might have been some measurement error. Another reason could be the higher yield stress of the material applied in Meppen compared to the yield stress in the numerical model, which is based on 16MND5.

7. Conclusions

A creep and material data base has been developed from the uniaxial tensile and creep tests of the REVISA program for the French 16MND5 steel. It is validated that the code simulates each uniaxial creep test (1D-problem) conservative and calculates mostly a close to experiment failure time.
The numerical creep and plasticity model has been applied to 2 tube-failure (2D-problem) experiments at different scales and of nominal different steels. The RUPTHER-14 and the "MPA-Meppen"-experiment. The comparison shows that not all effects can be represented by the numerical model, but the reason might not be the different kinds of steels rather than temperature effects in the experiments or different heats of the same steel. This assumption has to be investigated further.
An application of the numerical model to the 3D-experiment EC-FOREVER-2 has been performed, but will be improved. Also an extension to other 3D-problems is planed.

8. References

/ALT 2000/ E. Altstadt, Th. Moessner. *Extension of the ANSYS® creep and damage simulation capabilities.* Report, FZR-296, Forschungszentrum Rossendorf, Dresden, Germany, 2000.

/ANS 2001/ ANSYS®, Programmer's Manual, ANSYS®, Inc., 2001.

/CHU 1999/ T.Y. Chu, M.M. Pilch, J.H. Bentz, J.S. Ludwigsen, W.Y. Lu, L.L. Humphries: *Lower Head Failure Experiments and Analyses.* Report, NUREG/CR-5582, SAND98-2047, Sandia National Laboratories, Albuquerque, NM, USA, 1999./IMA 2001/ M. Kadner, Prüfbericht Nr. A191/1, Chemical Analysis of a steel specimen, Dresden, 2001.

/IKO 1999/ Ikonen, K., Creep Model Fitting Derived from REVISA Creep, Tensile and Relaxation Measurements, Technical Report MOSES-4/99, VTT-Energy, Espoo, Finland, 1999.

/LEM 1996/ J. Lemaitre, *A Course on Damage Mechanics,* ISBN 3-540-60980-6, 2nd edition Springer-Verlag Berlin, Heidelberg, New York, 1996.

/MON 1999/ Ph. Mongabure, M. Desmet, *RUPTHER Test#14 - Rupture test at 1000°C and variable pressure 8 then 6 bars,* Report SEMT/LISN/RT/99-003/A, CEA, France, 1999.

/OBS 1988/ V.-D. Obst, A. Klenk, P. Julisch, K. Maile, *Versuche zum Versagen einer Hauptkühlmittelleitung infolge Kriechbruch unter hohem Systemdruck,* (Tests about the failure of a main feed line due to creep under high system pressure) Report MPA 1500 771, Stuttgart, Germany, 1988.

/REM 1993/ J.L. Rempe, S.A. Chávez, G.L. Thinnes, C.M. Allison, G.E. Korth, R.J. Witt, J.J. Sienicki, S.K. Wang, L.A. Stickler, C.H. Heath, S.D. Snow: *Light Water Reactor Lower Head Failure Analysis.* Report NUREG/CR-5642, Idaho Falls, 1993.

/SAI 1998/ C. Sainte Catherine, *Tensile and creep tests material characterization of pressure vessel steel (16MND5) at high temperatures (20 up to 1300°C),* Rapport SEMT/LISN/RT/98-009/A, CEA, France, (experimental data files), 1998.

/SEH 1999/ Sehgal, B.R., Nourgaliev, R.R., Dinh, T.N., Karbojian, A., FOREVER experimental program on reactor pressure vessel creep behaviour and core debris retention, Proceedings of the 15-th International Conference on Structural Mechanics in Reactor Technology (SMiRT-15), Seoul, Korea, August 15-20, 1999.

/THF 1997/ T.G. Theofanous, C. Liu, S. Additon, S. Angelini, O. Kymäläinen, T. Salmassi. In-vessel coolability and retention of a core melt Nucl.Eng. Des. 169 1-48 1997

/WIL 2001/ H.-G. Willschütz, E. Altstadt, B.R. Sehgal, and F.-P Weiss: *Coupled thermal structural analysis of LWR vessel creep failure experiments,* NUCLEAR ENGINEERING AND DESIGN, vol 208, pp 265-282, 2001.

9. Acknowledgement

This work has been funded by the German Ministry of Economics BMWi under Contract No. 150 12 54.
The FOREVER experiments are performed under the sponsorship of the ARVI Project of the 5th-Framework Programme of the EU and the APRI Project jointly supported by SKI, Swedish and Finish Power Companies, USNRC, and HSK.
This work is supported by the ARTHUR UND AENNE FEINDT-STIFTUNG, Hamburg.

10. Appendix

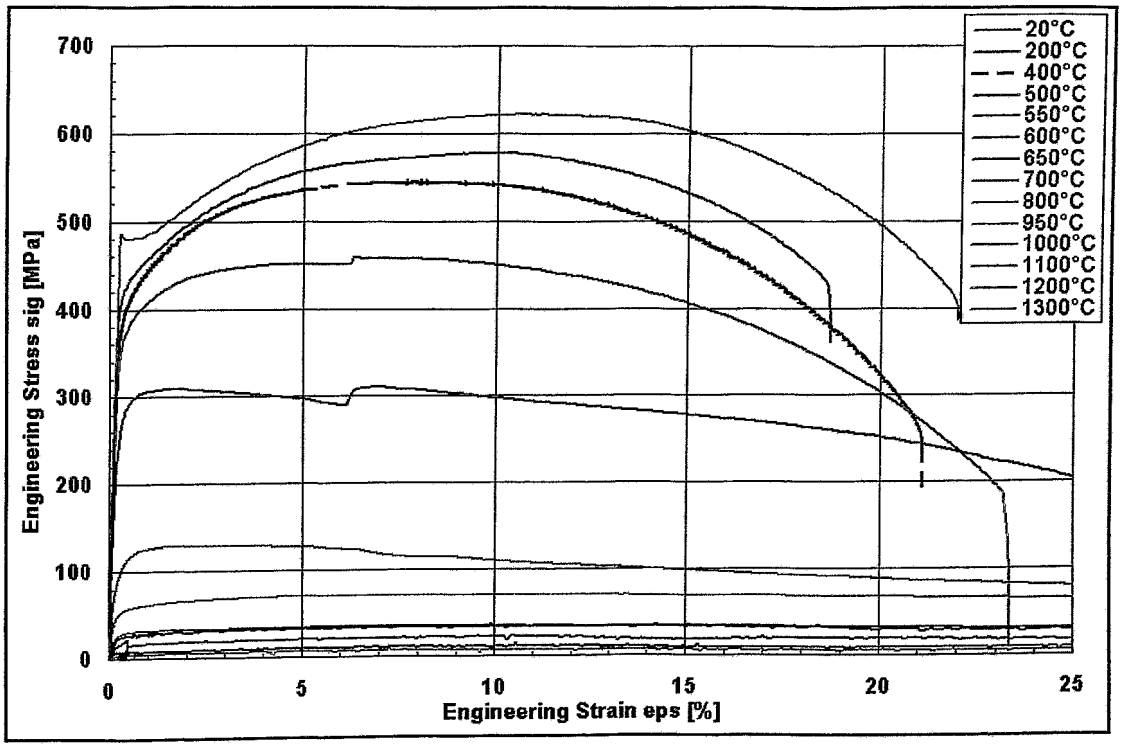

Figure 18: Engineering stress-strain curves of 16MND5 (REVISA-tests).

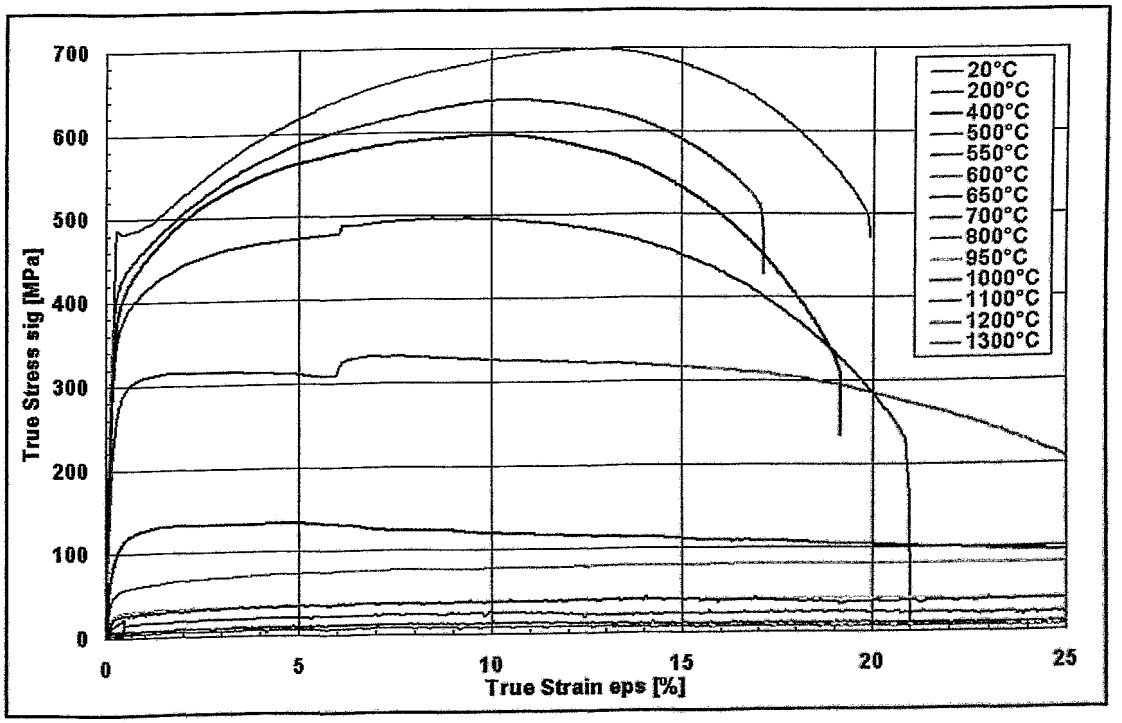

Figure 19: True stress-strain curves of 16MND5 (REVISA-tests).

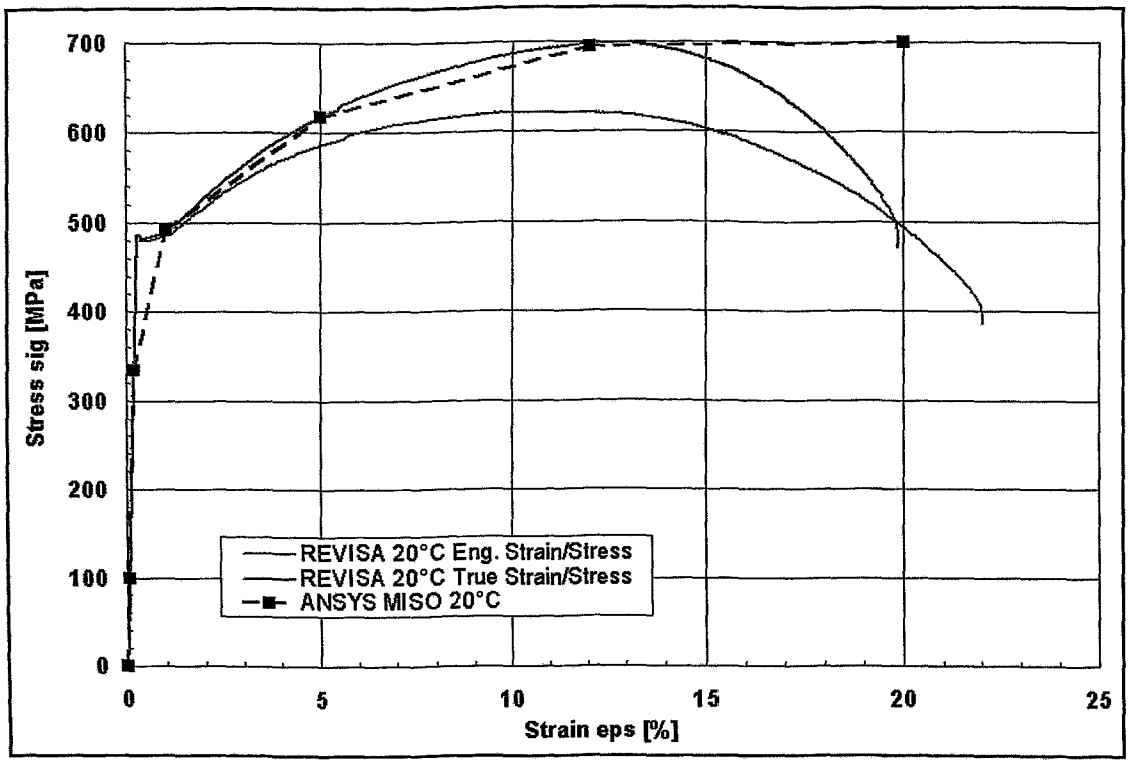

Figure 20: Measured and modeled Stress-strain relations at 20°C.

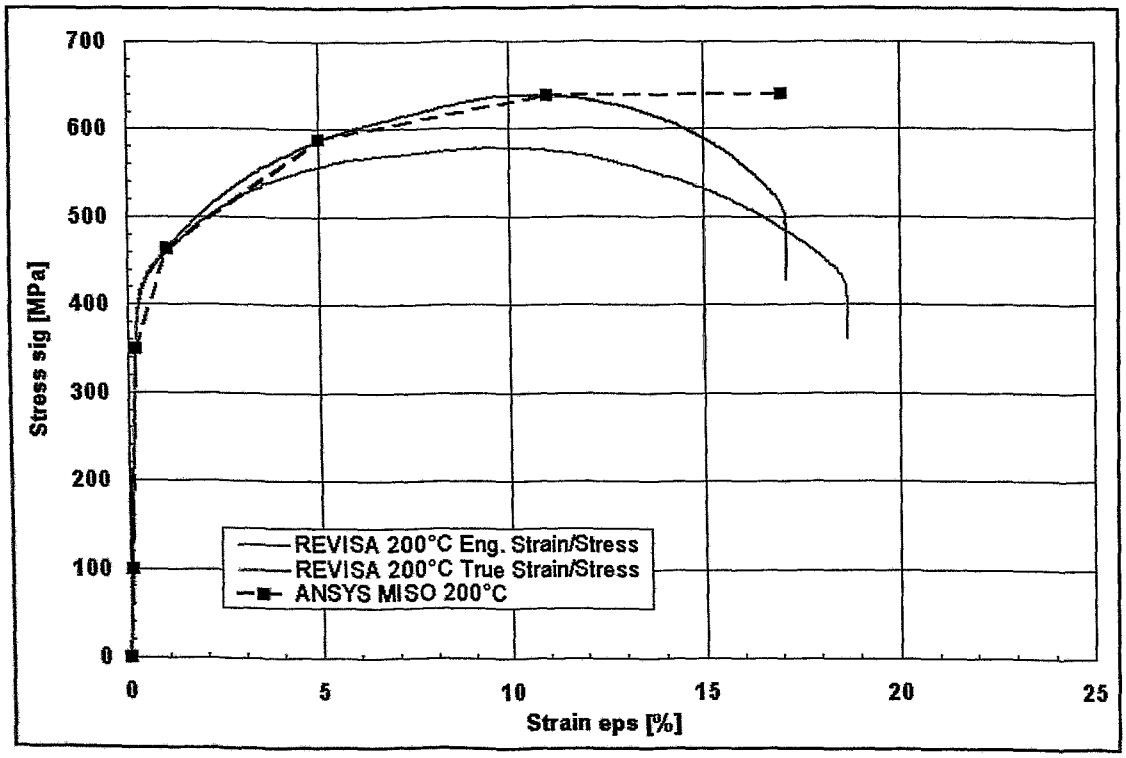

Figure 21: Measured and modeled Stress-strain relations at 200°C.

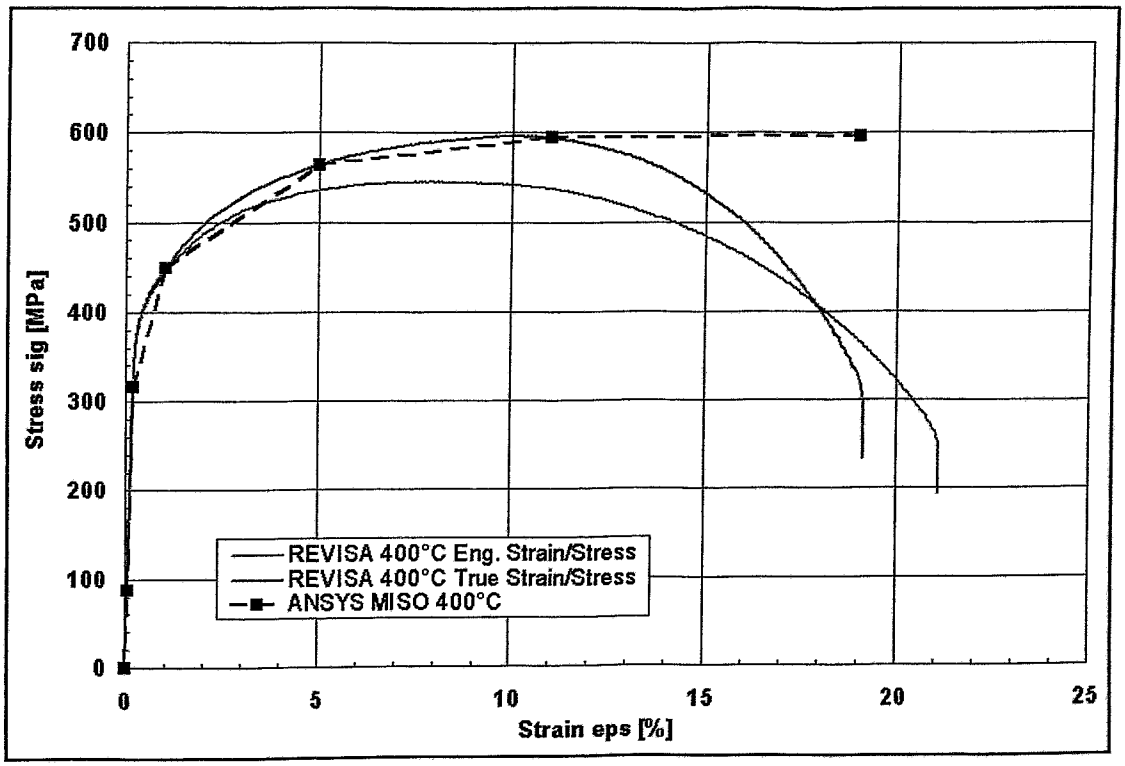

Figure 22: Measured and modeled Stress-strain relations at 400°C.

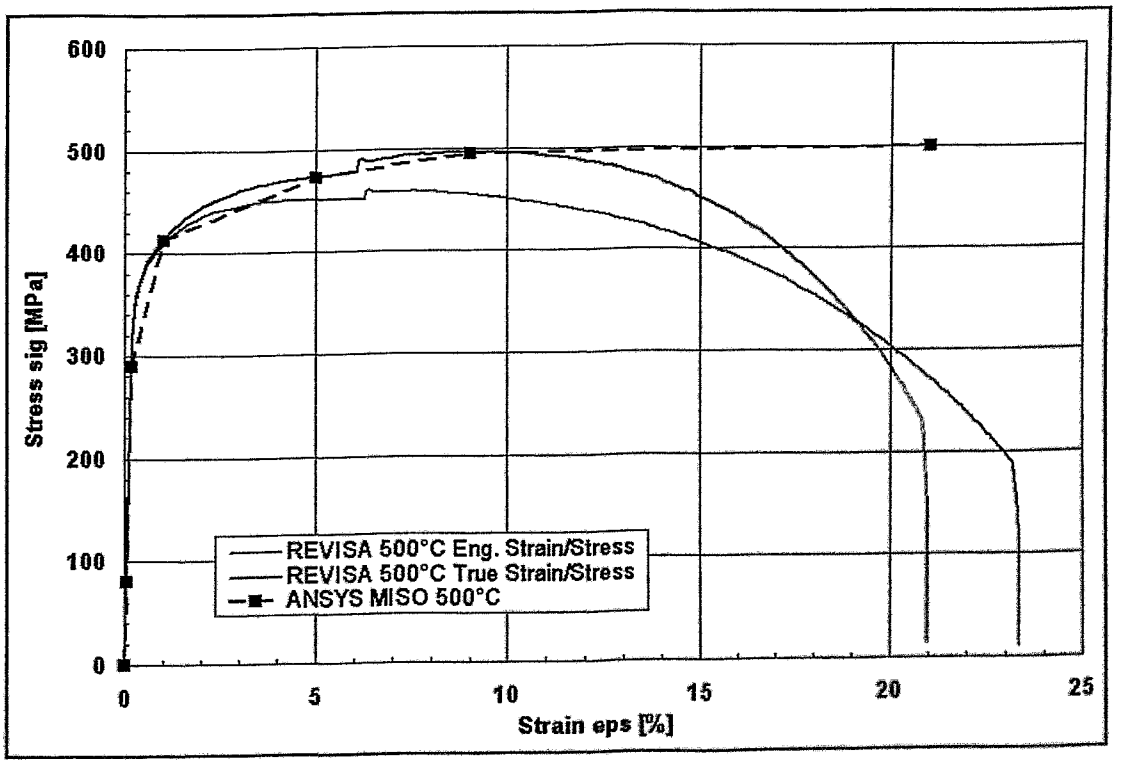

Figure 23: Measured and modeled Stress-strain relations at 500°C.

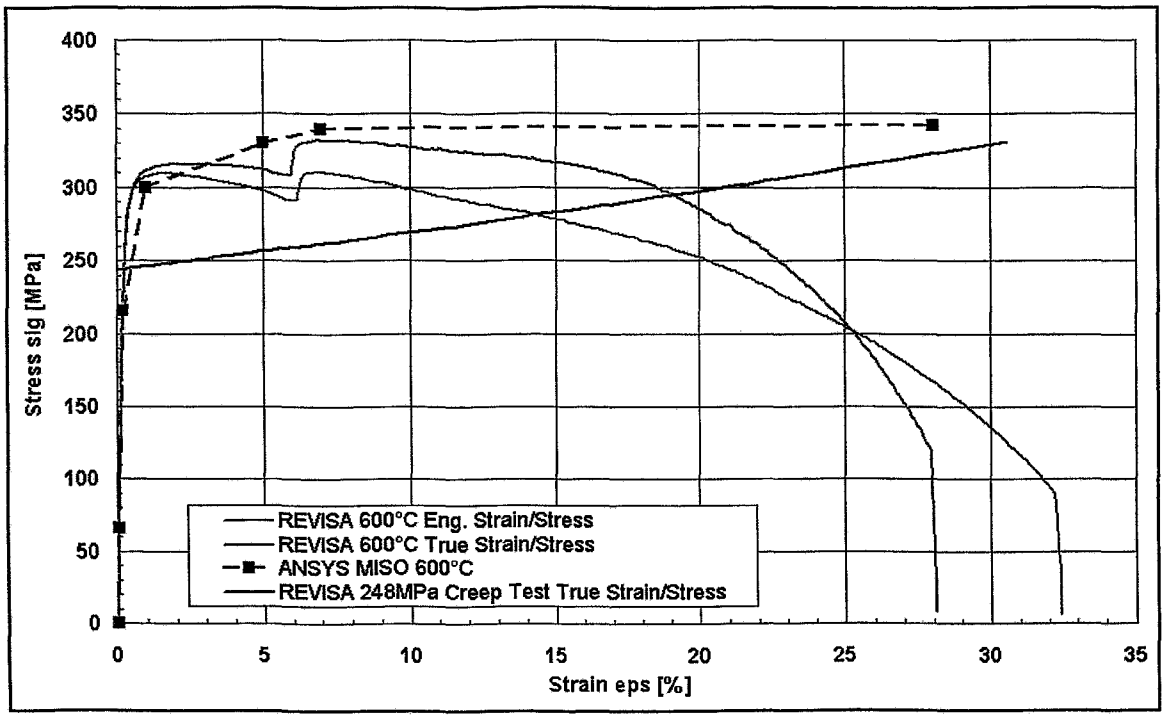

Figure 24: Measured and modeled Stress-strain relations at 600°C.

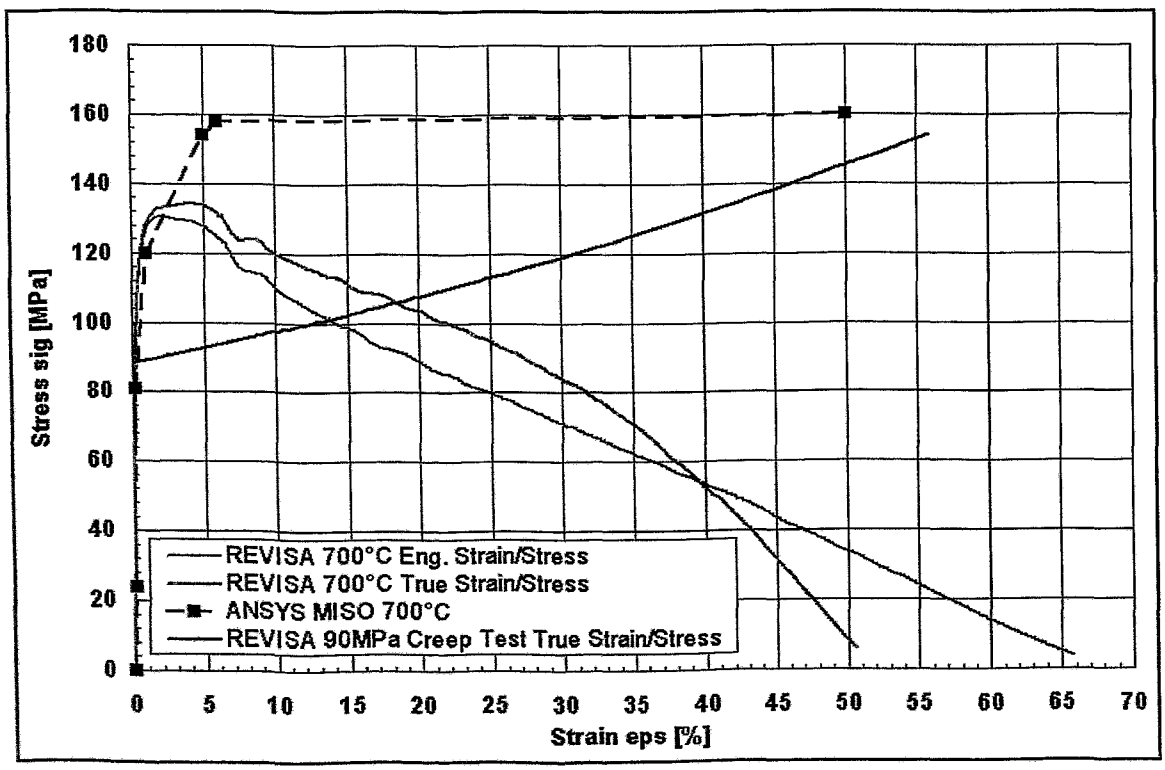

Figure 25: Measured and modeled Stress-strain relations at 700°C.

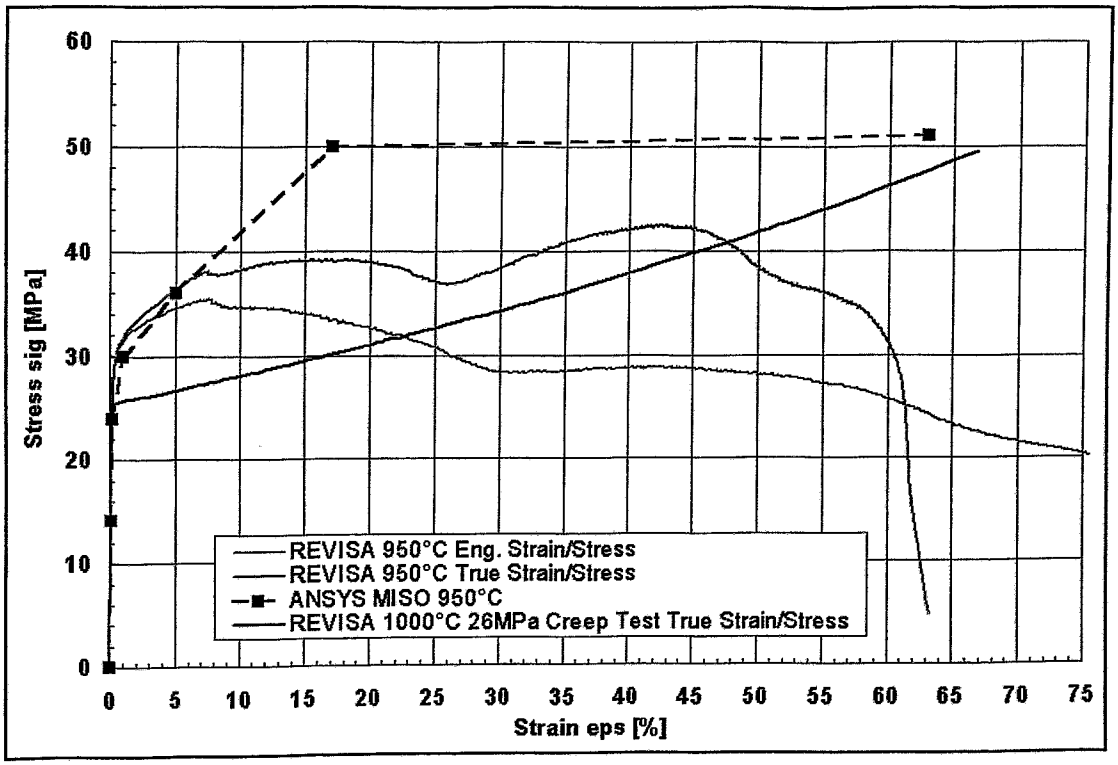

Figure 26: Measured and modeled Stress-strain relations at 950°C.

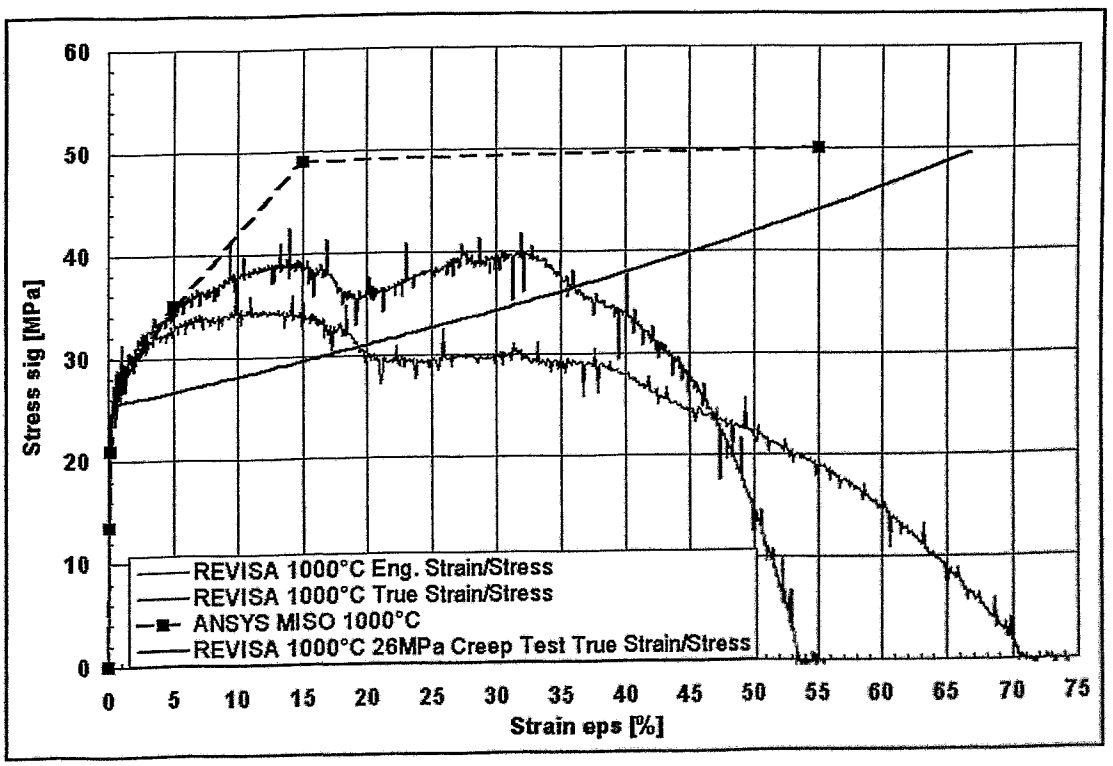

Figure 27: Measured and modeled Stress-strain relations at 1000°C.

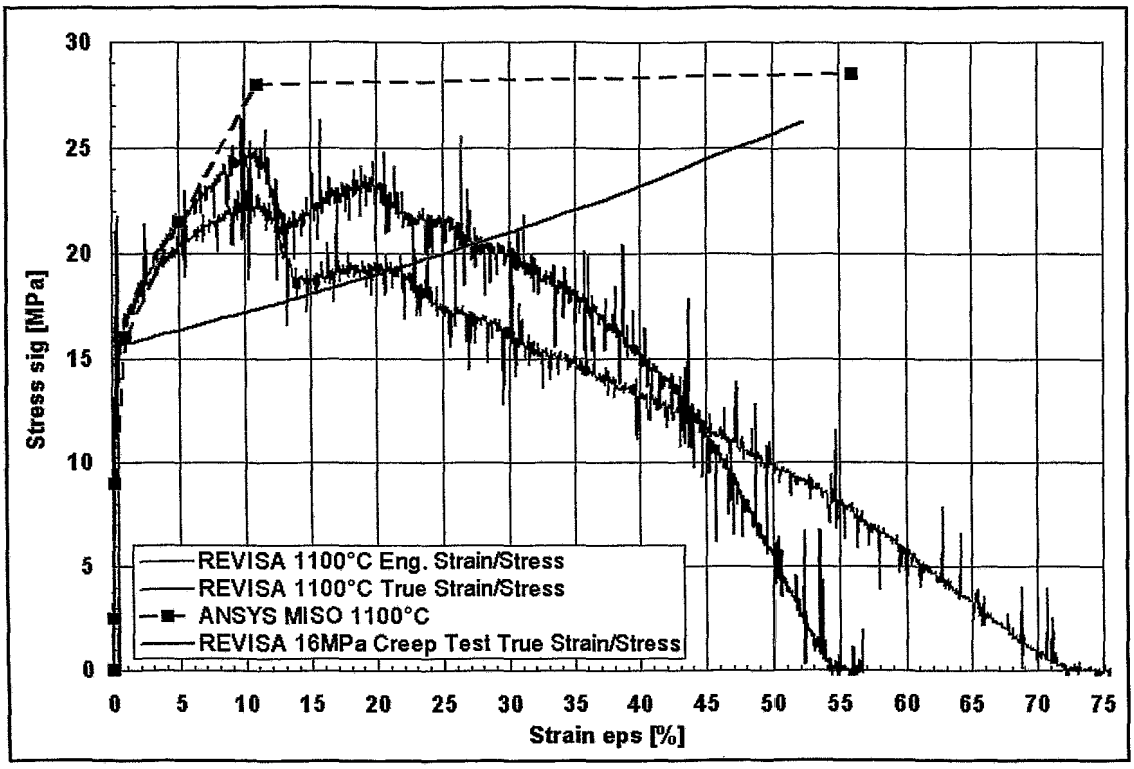

Figure 28: Measured and modeled Stress-strain relations at 1100°C.

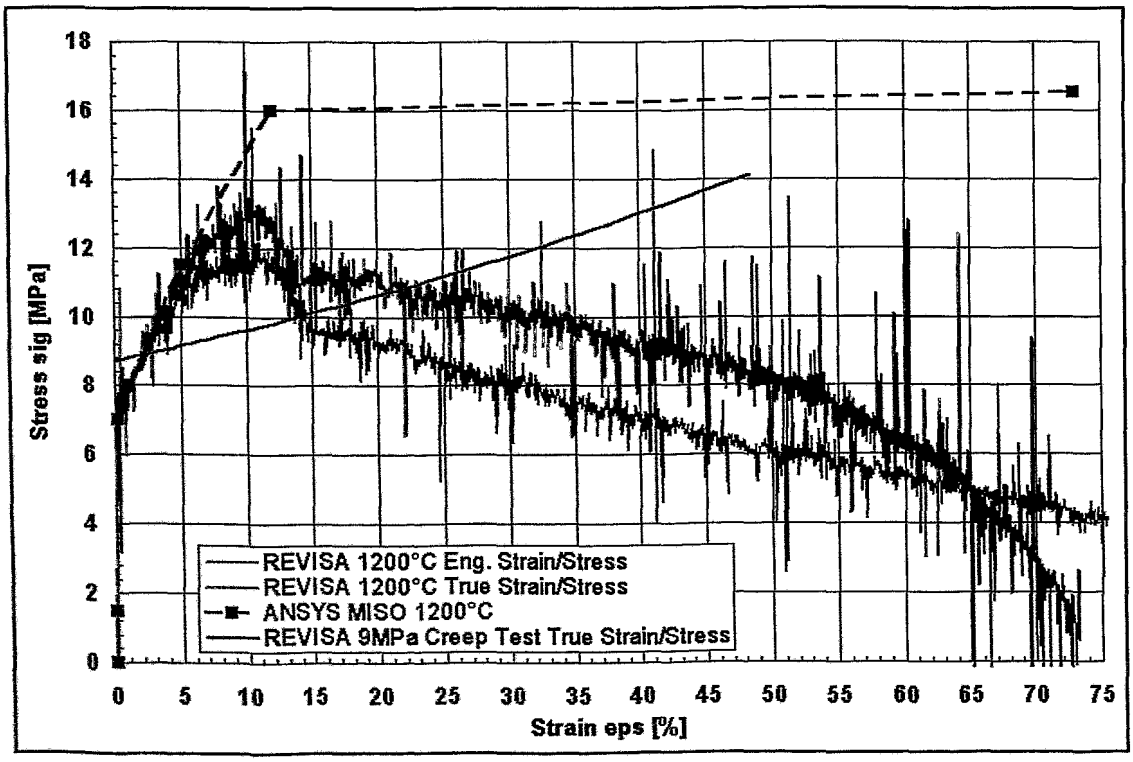

Figure 29: Measured and modeled Stress-strain relations at 1200°C.

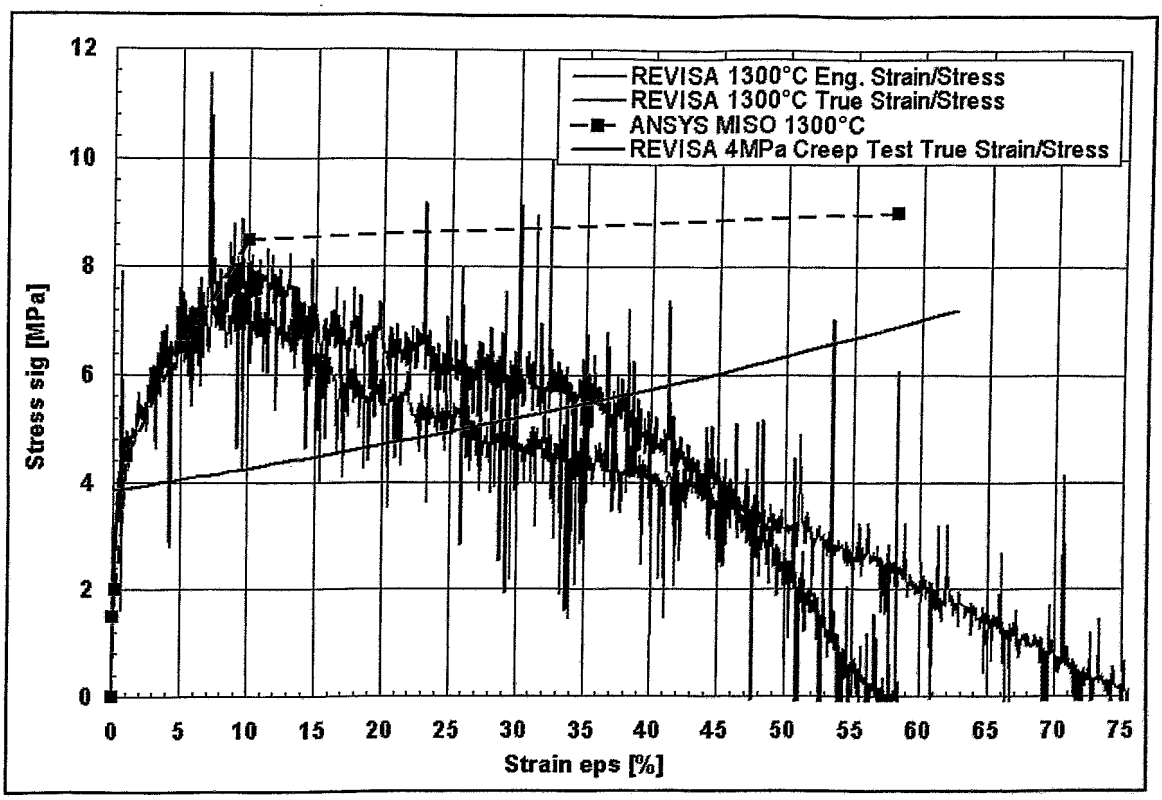

Figure 30: Measured and modeled Stress-strain relations at 1300°C.

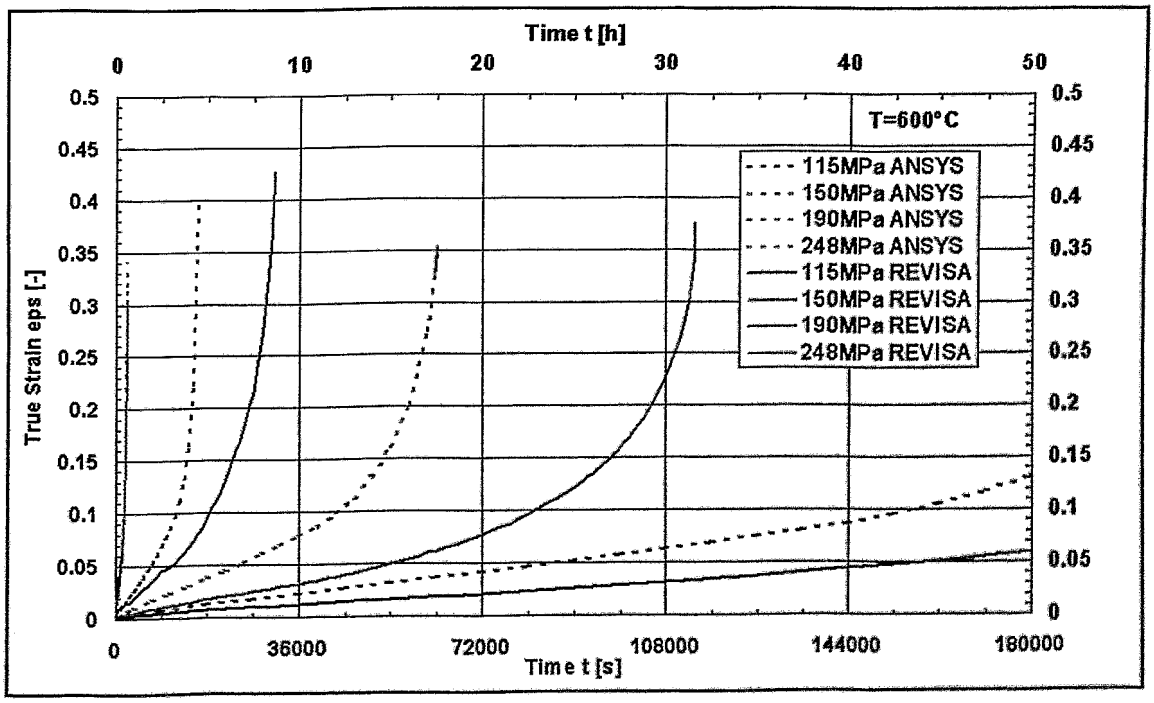

Figure 31: Comparison of uniaxial creep tests and calculation at 600°C.

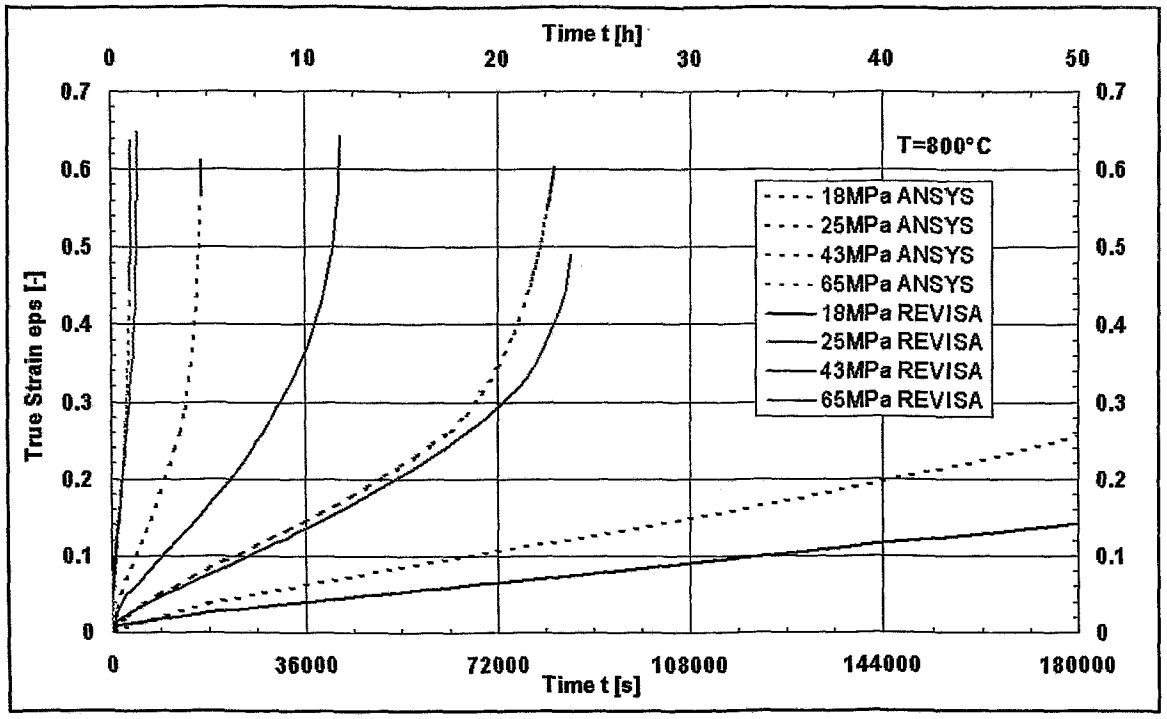

Figure 32: Comparison of uniaxial creep tests and calculation at 800°C.

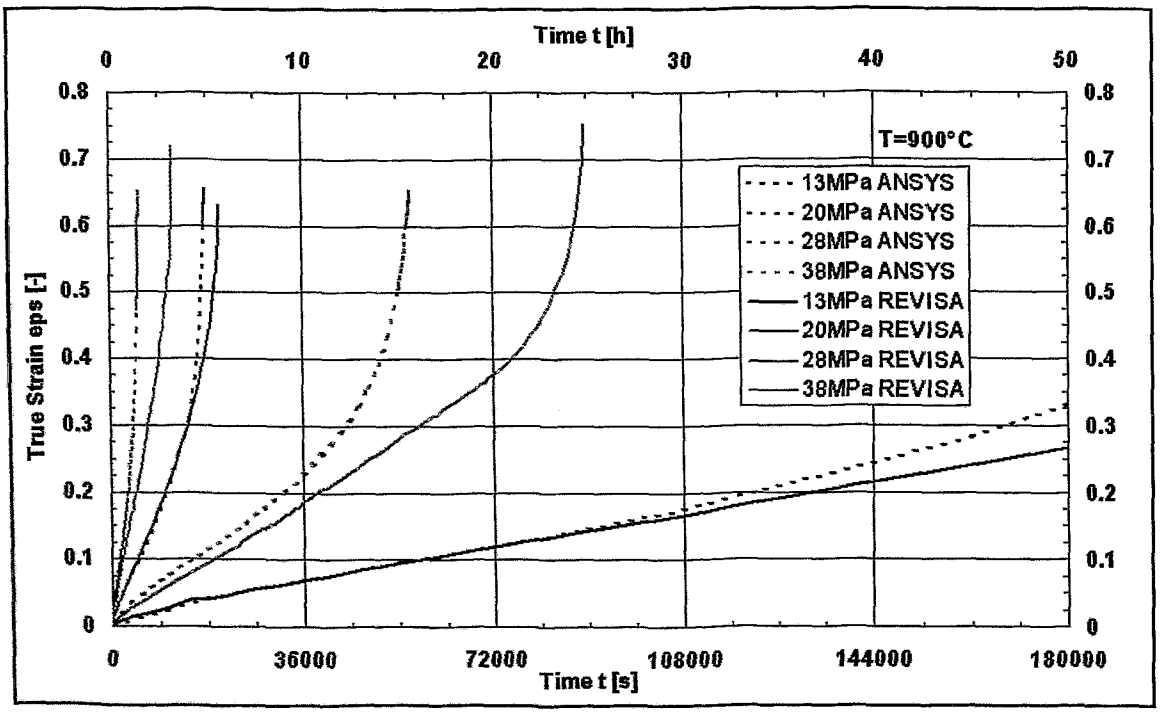

Figure 33: Comparison of uniaxial creep tests and calculation at 900°C.

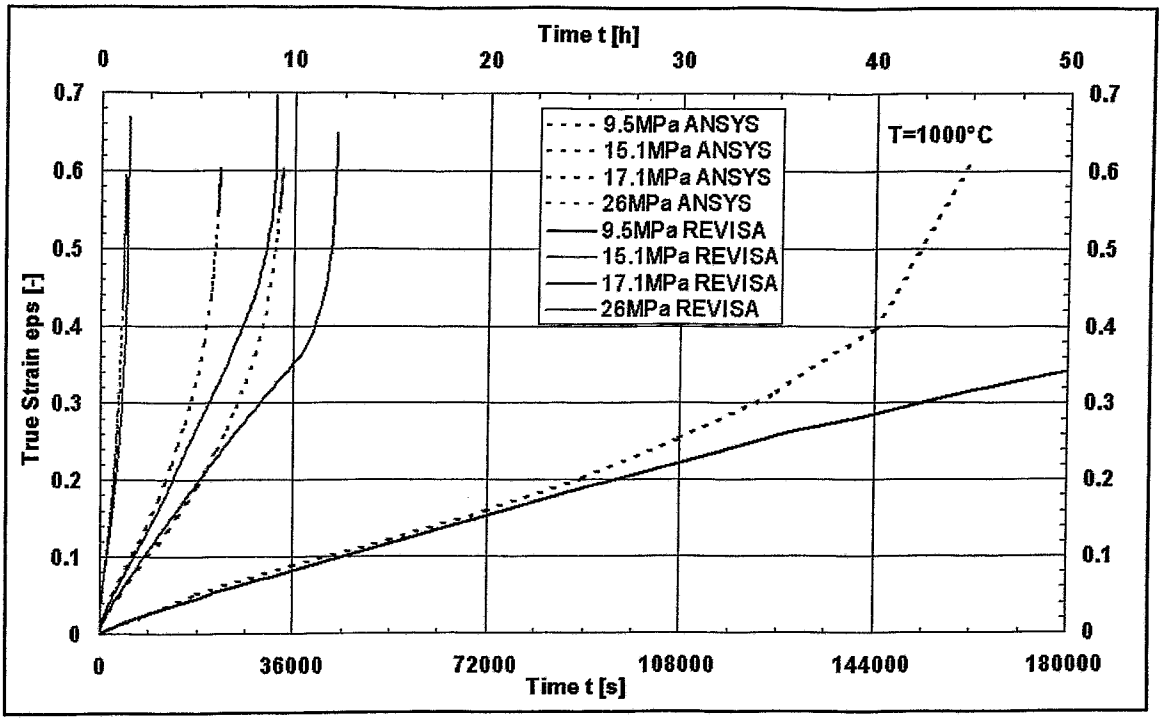

Figure 34: Comparison of uniaxial creep tests and calculation at 1000°C.

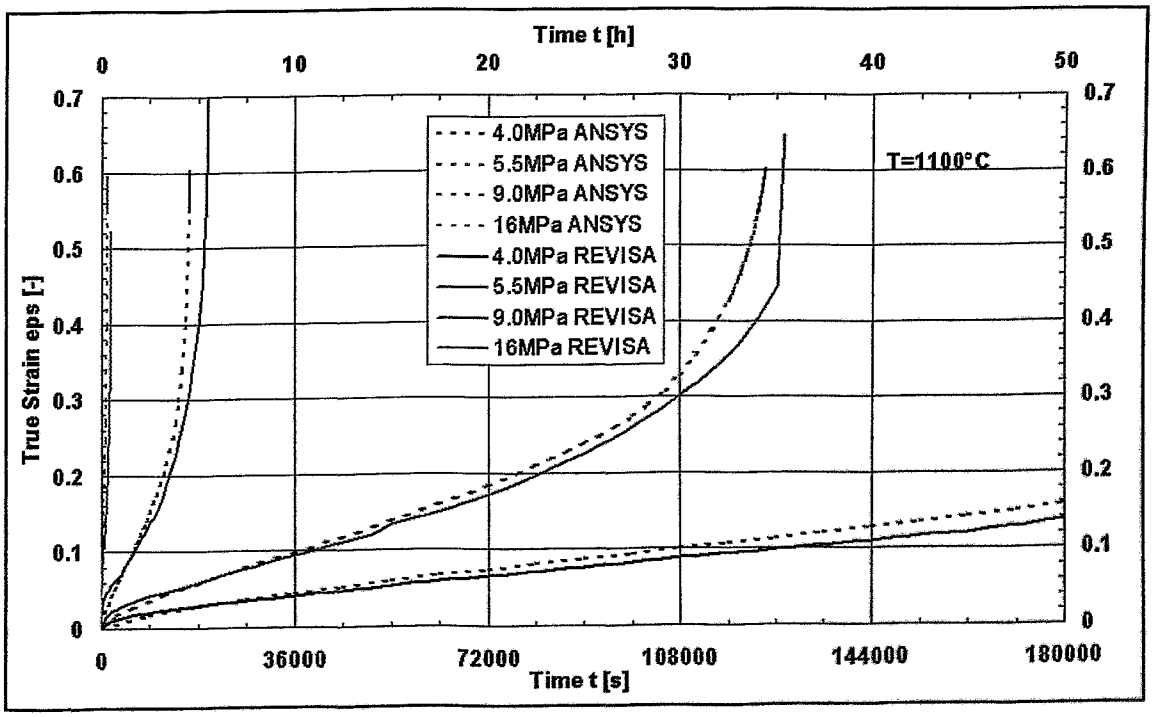

Figure 35: Comparison of uniaxial creep tests and calculation at 1100°C.

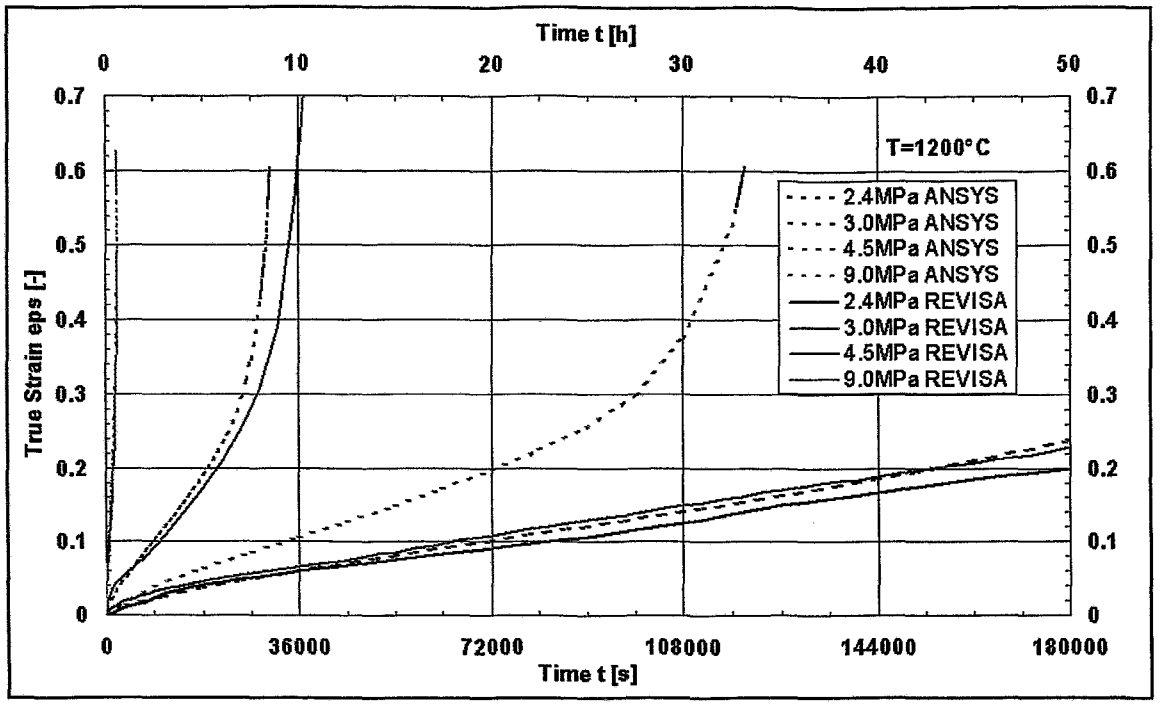

Figure 36: Comparison of uniaxial creep tests and calculation at 1200°C.

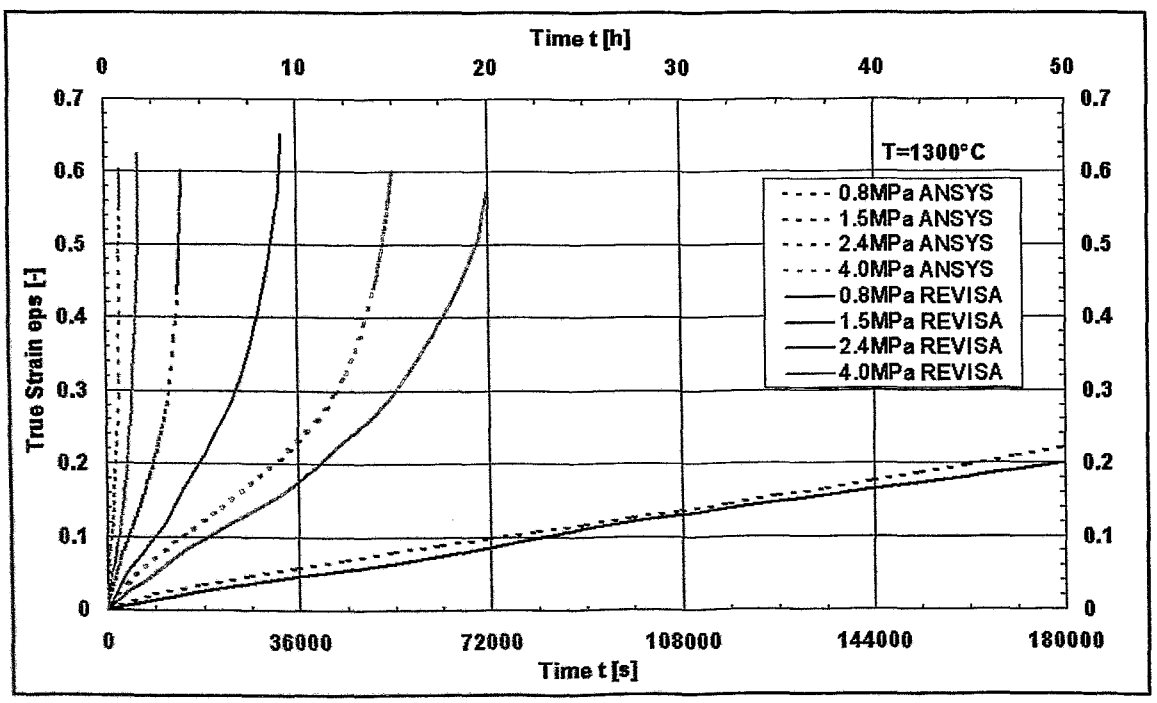

Figure 37: Comparison of uniaxial creep tests and calculation at 1300°C.